Cerebellar modulation of fear behaviour and memory encoding in the PAG.

Authors: *#Lawrenson CL[1], *#Paci E[1], Pickford J[1], Drake RAR[1], Lumb BM[1], Apps R[1]

Affiliation: [1] School of Physiology, Pharmacology and Neuroscience, University of Bristol, UK

Contributions: *Joint first author.

Corresponding authors.

Abstract:

The pivotal role of the periaqueductal grey (PAG) in fear learning is reinforced by the identification of neurons in rat ventral PAG (vPAG) that encode fear memory through signalling the onset and offset of an auditory conditioned stimulus during presentation of the unreinforced conditioned tone during retrieval. Some units only display CS+ onset or offset responses and the two signals differ in extinction sensitivity, suggesting they are independent of each other. In addition, understanding cerebellar contributions to survival circuits is advanced by the discovery that: (i) reversible inactivation of the medial cerebellar nucleus (MCN) during fear consolidation leads in subsequent retrieval to: (a) disruption of the temporal precision of vPAG offset, but not onset responses to the unreinforced conditioned tone, and (b) an increase in duration of freezing behaviour. And (ii) chemogenetic manipulation of the MCN-vPAG projection during fear acquisition: (a) reduces the occurrence of fear-related ultrasonic vocalisations and (b) during subsequent retrieval, slows the extinction rate of fear-related freezing. These findings show that the cerebellum is part of the survival network that regulates fear memory processes at multiple timescales and in multiple ways; raising the possibility that dysfunctional interactions in the cerebellar-survival network may underlie fear-related disorders and comorbidities.

Impact Statement:

Cerebellar-periaqueductal grey interactions contribute to fear conditioned processes and, as such, provide a novel target for treating psychological conditions including post-traumatic stress disorder.

UOB Confidential

Introduction

The periaqueductal grey (PAG) lies at the hub of central networks that co-ordinate survival, including coping behaviours mediating defensive and fear-evoked coping responses. Neurons in the functionally distinct longitudinal columns of the PAG co-ordinate different aspects of survival behaviours. Of particular relevance to the current study, fear-evoked freezing is mediated by neurons in its ventrolateral sector (Vianna et al., 2001; Walker et al., 2003; Tovote et al., 2016; Watson et al., 2016). Fear-related behaviours co-ordinated by the PAG also extend to the expression of 22kHz ultrasonic vocalizations (USVs; Kim et al., 2013; Ouda et al., 2016) and risk assessment activity such as rearing (Sandner et al., 1987; Clelland et al., 2010). Furthermore, at a cellular level, electrophysiological studies have found that neurons in ventrolateral PAG encode associatively conditioned fear memory (Watson et al., 2016; Wright et al., 2019).

Central nervous system survival networks involving the PAG are well documented (Carrive et al., 1997; Vianna et al., 2001; Walker et al., 2002; Tovote et al., 2015; Watson et al., 2016; Ozawa et al., 2017). Until recently, the cerebellum was generally considered not to be part of this network. However, there is good evidence in cats and rodents that vermal regions of the cerebellum contribute to motor and autonomic components of defensive states: inactivation of vermal cerebellar cortex (lobules IV-VIII), or one of its main output nuclei (medial cerebellar nucleus, MCN, aka fastigial nucleus), leads to deficits in fear-related behaviours such as context conditioned bradycardia (Supple et al., 1990); the expression of innate fear (Supple et al., 1987; Koutsikou et al., 2014); and fear conditioned freezing behaviour (Asdourian et al., 1970; Sacchetti et al., 2002, 2005; Koutsikou et al., 2014). In addition, the emission of USVs has been related to cerebellar function (Fujita et al., 2008; Fujita-Jimbo et al., 2014; Toledo et al., 2019), and inactivation of the cerebellar vermis during innate and conditioned fear unmasks risk assessment rearing behaviour (Koutsikou et al., 2014).

The cerebellum is reciprocally connected to many brain regions associated with survival networks (Sacchetti et al., 2009; Strick et al., 2009; Apps & Strata, 2015) and in all mammalian species studied so far (cat, rabbit, rat, mouse, human), this includes interconnections with the ventrolateral PAG (Whiteside et al., 1953; Teune et al., 2000; Nisimaru et al., 2013; Koutsikou et al., 2014; Cacciola et al., 2019; Vaaga et al., 2020; Frontera et al., 2020). Thus, the dependence of survival behaviours on the integrity of the cerebellum, together with reciprocal connections between the ventrolateral PAG and the cerebellum raise the possibility of an important role of cerebellar interactions with the PAG in the expression of such behaviours.

UOB Confidential

An emerging concept is that the cerebellar vermis and its output nucleus MCN are involved in the control of an integrated array of fear-related functions, including fear memory and fear-induced behaviours such as freezing and their extinction (Sacchetti et al., 2002, 2005; Koutsikou et al., 2014; Utz et al., 2015). Important insights into the role of the murine MCN-ventrolateral PAG pathway in modulating PAG fear learning and memory have been provided recently (Vaaga et al., 2020; Frontera et al., 2020). However, it is not known whether PAG neural encoding of fear memory is dependent on the integrity of its cerebellar input. More generally, given the well-established role of the cerebellum in the co-ordination of movements and in particular, the representation of temporal relationships (e.g. Xu et al., 2006; Koch et al., 2007; Bares et al., 2007; Spencer & Ivry, 2013) it remains to be determined whether the cerebellum enables the survival circuit network to elicit behaviourally appropriate responses at different times during fear conditioning. Effects during retrieval and subsequent extinction of a fear conditioned response are of particular interest because deficits in extinction processes are thought to underly psychological conditions such as post-traumatic stress disorder (Bremner et al., 1999; Herry et al., 2010; Milad et al., 2012) and have also been related to chronic pain phenotype (Ji et al., 2018).

The experiments reported here used a combination of electrophysiological, behavioural and interventionist approaches in an auditory cued fear conditioning paradigm in rats to interrogate the role of MCN interactions with the PAG in the expression of fear-related behaviours. Our main findings are that: (i) PAG encodes temporally precise information about the onset and offset of a fear conditioned stimulus and that these two neural signals may be generated by independent mechanisms; (ii) both onset and offset responses correlate with fear related freezing behaviour; (iii) MCN is part of a larger circuit that regulates the temporal accuracy of PAG encoding of fear conditioned stimulus offset but not onset during retrieval of a conditioned response; (iv) MCN is involved in distinct aspects of survival behaviour at different times during fear conditioning: during acquisition the emission of USVs and subsequent rate of extinction of conditioned freezing during retrieval. While during consolidation, its influence on survival circuits effects the duration of conditioned freezing in subsequent retrieval. In summary, the present study provides evidence that the cerebellum through its interactions with survival circuits regulates the ability of the PAG to encode a fear memory trace with temporal precision and also regulates the timing of appropriate patterns of behaviour during fear acquisition and retrieval.

UOB Confidential

Results

vPAG neuronal responses during an auditory cued fear conditioning paradigm

As a first step, an auditory cued fear conditioning paradigm (Fig. 1A) was used to investigate how single unit activity in the PAG responded to fear acquisition and subsequent retrieval and extinction of fear conditioned responses (n = 10 animals total; n = 6 with dual microdrives and n = 4 microdrives combined with cannulae, see Methods for details and Fig. 1B-E). In all animals the position of tetrodes was histologically verified. The majority of PAG tetrode recording sites were located in the ventral sector of the PAG (Supplementary Fig. 1).

UOB Confidential

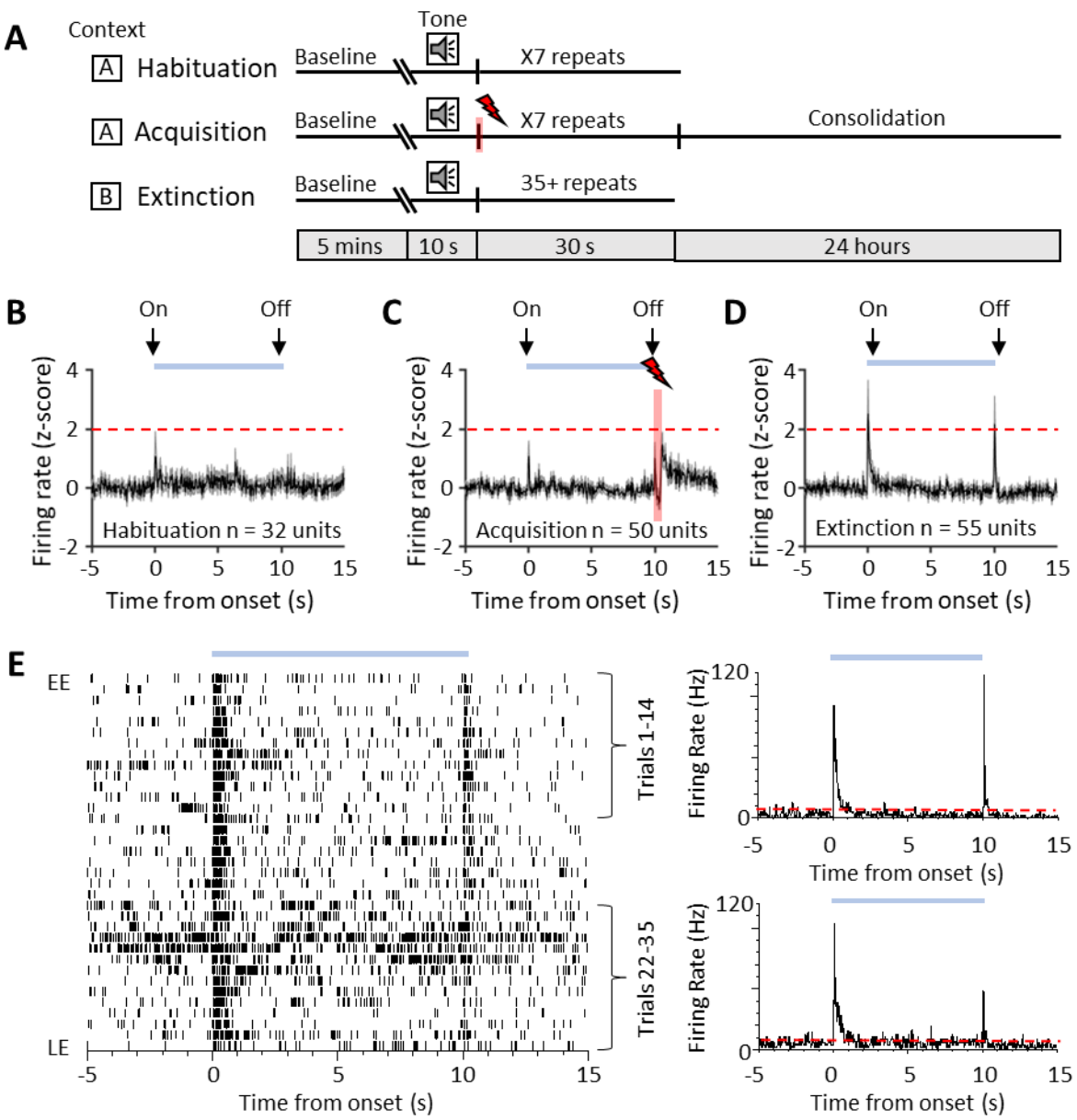

Figure 1. Single unit vPAG responses during auditory cued fear delay conditioning. (A) Schematic representation of the fear conditioning paradigm composed of habituation, acquisition and extinction sessions. Habituation and acquisition were carried out in context A, whilst extinction training was in context B. During acquisition, a CS tone was paired with a US footshock (see Methods for details). (B) Peri event time histogram (PETH) showing average firing rate of all available single units (n = 32) recorded during presentation of the unconditioned tone (10s) during habituation in control animals. Time zero, tone onset. Light blue bar shows time the tone is on. (C) Same as B but all available single units (n = 50) recorded during acquisition (shaded red and lightening symbol indicate time of US footshock when the stimulus artefact prevented neural recording). (D) Same as B but all available single units (n = 55) recorded during presentation of the unreinforced CS+ during extinction. For B-D, individual unit activity was z-score normalised to a 5 second baseline before tone onset. Horizontal dashed red line represents significance level ($p<0.05$). PETHs show mean ± SEM; 40ms bins. (E) Example type 1 onset and offset single unit recorded during extinction training. Data displayed as raster plot

UOB Confidential

from early extinction (EE) to late extinction (LE) with corresponding PETH for EE (trials 1-14) and LE (trials 22-35) (40ms bins, time zero onset of CS+. Horizontal dashed red line represents significance level ($p < 0.05$).

UOB Confidential

A total of 32 vPAG units were recorded during habituation (Fig. 1 B). The majority (75 %, n = 24/32 units) were unresponsive to the unconditioned auditory tone; the remainder responded (see Methods for definition) to tone onset (either increasing, n = 6/32 units or decreasing firing rate, n = 2/32 units); and in some of these cases (15.6 %) also to tone offset (either increasing 3/32 units or decreasing firing rate 2/32 units).

We recorded the activity of 50 vPAG units during acquisition where the CS tone was paired with the US footshock at tone offset (Fig. 1C). Some of these units (18.5 %) responded to CS onset. Following the US, 20 % of the total also displayed an increase in firing rate which presumably reflects sensory afferent drive to the PAG as a result of the aversive peripheral stimulus (e.g. Sanders et al., 1980; Heinricher et al., 1987; Sharma et al., 1999). Across all recorded units, the average increase in activity following the US was not statistically significant (Fig. 1C, z-score < 1.96).

During retrieval and extinction of the conditioned response we recorded a total of 55 vPAG units. Retrieval is defined here as early extinction (EE) training when the unreinforced CS+ reliably elicits a conditioned response. In retrieval 29 units (52.7 %) displayed a transient increase in activity during presentation of the unreinforced conditioned stimulus (CS+, Fig. 1D, E). In keeping with a previous classification of PAG unit activity during fear-conditioned extinction training (Watson et al., 2016) these units are therefore defined as type 1. The pattern of response was typically a phasic increase in activity at CS+ onset but an additional feature not previously reported for vPAG units was a phasic increase in activity at CS+ offset (Fig. 1D, E). A total of 21/29 (72.4 %) type 1 units responded to both CS+ onset and CS+ offset, while 3/29 units (10.3 %) only responded to CS+ onset and 5/29 units only responded to CS+ offset (17.3 %). This raises the possibility that CS+ onset and offset responses may be mediated by separate mechanisms. We have therefore termed them type 1 onset and type 1 offset responses, respectively.

Of the remainder of the sample of vPAG units recorded in control animals during EE, 22 units (40 %) demonstrated no significant change in firing rate and were therefore defined as type 2 (Watson et al., 2016). Four units (7 %) responded to CS+ onset with a decrease in firing rate (2 of these units also reduced their firing rate at CS+ offset) and therefore were classed as type 4. No type 3 units (biphasic response) were observed.

Since the majority of responsive vPAG units recorded in control experiments were type 1 (i.e. displayed an increase in firing rate) the following analysis is confined mainly to consideration of their activity during fear conditioned retrieval and extinction. The majority of type 1 onset units (75 %, 18/24 units) and type 1 offset units (73 %, 19/26 units) showed a significant reduction in responsiveness during extinction training, as measured by the integrated area of response during CS+

UOB Confidential

trials in EE versus late extinction (LE, Fig. 2B, D, control, type 1 onset units: $p < 0.0001$, paired t-test; type 1 offset units, Fig. 2F, H, $p = 0.0003$, paired t-test). For type 1 onset responses this reduction was not evident for mean peak z-score (Fig. 2E, decrease of 13.8 % from EE to LE; paired t-test; $p = 0.197$) but was evident for type 1 offset responses (Fig. 2I, decrease of 67.0 % from EE to LE; paired t-test; $p = 0.011$). This distinction between onset and offset responses provides additional evidence that they may be evoked by separate mechanisms.

UOB Confidential

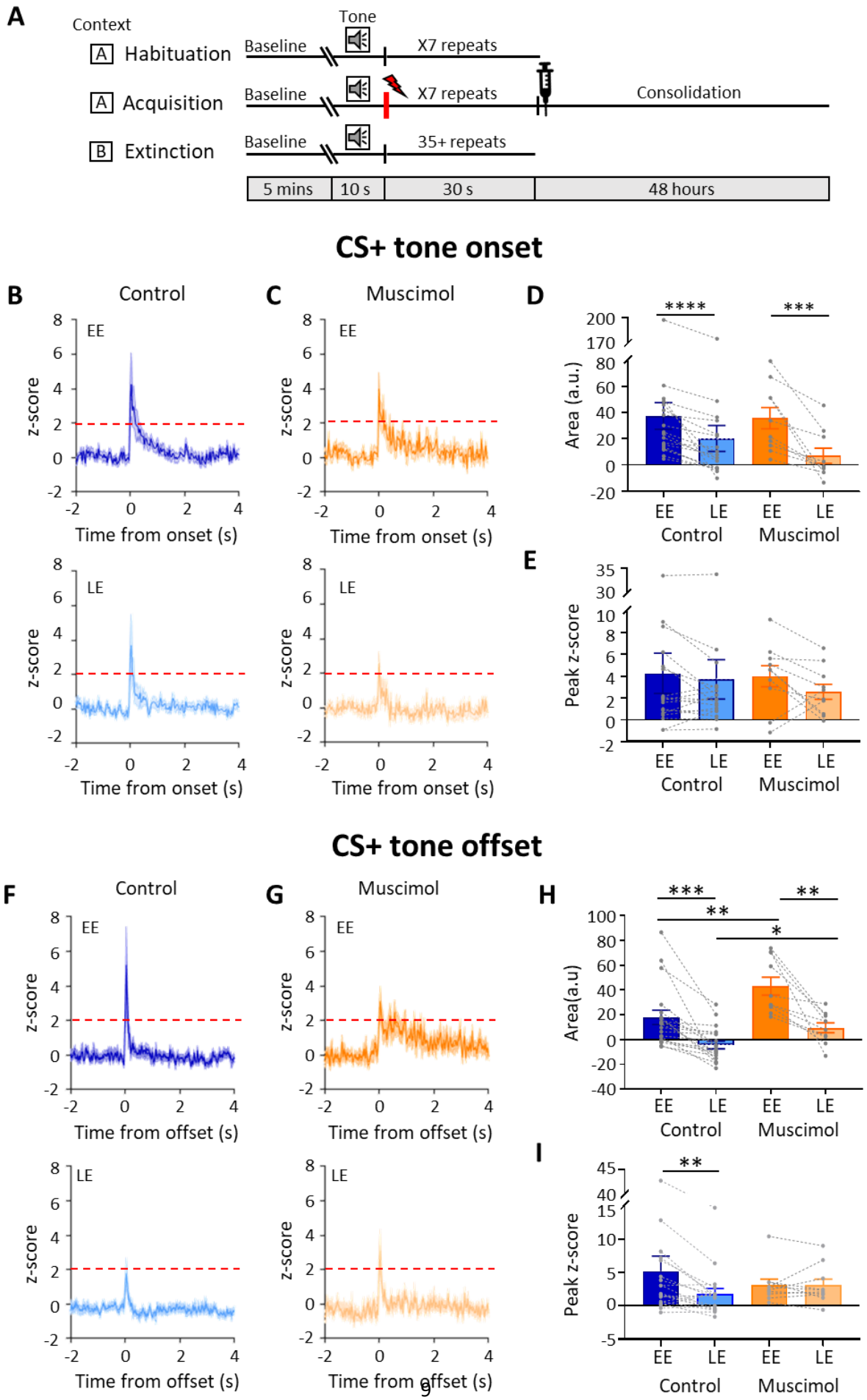

1

UOB Confidential

Figure 2. Effect of MCN inactivation during consolidation on vPAG type 1 onset and offset responses during extinction. A) Schematic timeline representing the fear conditioning protocol for muscimol animals. B) Group data for control animals showing average z-scored type 1 onset responses (n = 18 units) during early extinction (EE, upper panel) and late extinction (LE, lower panel); solid lines in each plot show mean z-score, shaded regions ± SEM; horizontal dashed red lines show significance level ($p<0.05$). Time zero, CS+ tone onset (C) Same as B but grouped data for muscimol animals (n = 10 single units). (D) Bar charts showing average type 1 onset response area (arbitrary units) during EE and LE for single units recorded in control versus muscimol animals. Pairs of data points connected with dashed lines show change in mean response area for each single unit over extinction training. Bars show group means ± SEM. Paired t-test, **** $p < 0.0001$, *** $p < 0.001$. (E) Same as D but grouped data for peak z-score. (F) Same as B but control type 1 offset responses (n = 19 single units) during EE (upper panel) and LE (lower panel). Time zero, CS+ tone offset. (G) Same as F but grouped data for muscimol animals (n = 10 single units). (H) Same as D but showing average type 1 offset response area (arbitrary units) during EE and LE for single units recorded in control versus muscimol animals. Paired t-test, *** $p < 0.001$, ** $p < 0.01$; Unpaired t-test, ** $p < 0.01$, * $p < 0.05$. H) Same as I but grouped data for peak z-score. Paired t-test, **$p < 0.01$.

vPAG offset responses during trace conditioning.

For the results described above, a delay classical conditioning paradigm was used where the unconditioned stimulus (US) was timed to occur at CS offset (Fig. 1A, see Methods). For the unit activity recorded at CS+ offset it was therefore unclear whether the change in firing rate during retrieval signals the end of the conditioned tone and/or represents the timing of the expected US. To examine this, in three animals, a 1 second trace interval was introduced between the CS and US during acquisition trials. A total of 6 type 1 units (those with increased activity at CS+ offset), were found to show a change in activity that was temporally related to the offset of the CS+ during retrieval and not to the time of the expected occurrence of the US (1s after CS+ offset, Supplementary Fig. 3A, B). We also recorded 6 units with type 4 responses (those with reduced activity at CS+ offset) and in trace conditioning their activity was also related to time of CS+ offset (Supplementary Fig. 3C, D). A comparison of time to peak or trough of response for all available units recorded during control versus trace conditioning showed no statistical difference (Supplementary Fig. 3E; $p = 0.091$, unpaired t test). These results are therefore consistent with vPAG activity signalling the conditioned tone offset rather than a prediction of the timing of the unconditioned stimulus.

Population activity in the MCN and vPAG

It was also of interest to consider any changes in neural population activity during extinction training. To assess such changes, auditory event related potentials (ERPs) were recorded simultaneously from the MCN and vPAG, following a delay conditioning paradigm (n = 6 animals, Fig. 3). For vPAG we were able to compare the ERP waveform to the simultaneously recorded unit

UOB Confidential

activity and found that field duration and spike activity were broadly concomitant (Supplementary Fig. 4).

The ERP recorded in the vPAG at CS+ onset had a significantly shorter onset latency then the ERP recorded in the same animals in MCN (vPAG onset 6.0 ± 1.14ms; MCN onset 25.3 ± 2.43ms, $p = 0.006$, paired t-test). However, latency to peak was not significantly different (PAG peak 65.4 ± 1.4 ms; MCN peak 74.5 ± 6.6 ms, $p = 0.294$, paired t-test). At CS+ offset the ERP in the vPAG was also significantly shorter in latency than the ERP in MCN (vPAG offset 28.6 ± 6.3 ms; MCN offset 47.6 ± 2.7 ms, $p = 0.037$; paired t-test), while latency to peak was similar (vPAG peak 89.6 ± 5.7 ms; MCN peak 99.0 ± 6.5 ms, $p = 0.310$, paired t-test). The difference in onset latency between ERP responses recorded at CS+ onset and offset within both vPAG and MCN was statistically significant (vPAG onset vs offset, $p = 0.024$, Welch unpaired t-test; MCN onset vs offset, $p = 0.0003$, unpaired t-test). This difference suggests the ERP responses at CS+ onset and CS+ offset are likely to be generated by different neural pathways.

During extinction training, the peak-to-peak amplitude of the ERPs recorded in the MCN and vPAG at CS+ onset did not show a statistically significant difference (Fig. 3A, C, MCN: EE ERP 421.6 ± 126 mV vs LE ERP 309.3 ± 88.7 mV, $p = 0.115$, paired t-test; vPAG: EE ERP 501.1.2 ± 104.7mV vs LE ERP 418 ± 84.08 mV, $p = 0.313$, paired t-test). By comparison, ERPs recorded at CS+ offset in the vPAG (Fig. 3B, D) showed a significant decrease in amplitude during extinction training in EE versus LE (65% reduction in ERP size, EE 520.3 ± 124.7 vs LE 337.8 ± 96.29, $p = 0.007$, paired t-test), while in the MCN there was no significant decrease (EE 537.3 ± 173.2 vs LE 430.5 ± 135.6, $p = 0.074$, paired t-test). The differences found in vPAG between onset and offset ERPs provide further evidence that they are generated and regulated by different neural pathways.

To assess if changes in ERP amplitude during extinction covaried between MCN and vPAG, we compared average ERP amplitude at CS+ onset (Fig. 3E) and CS+ offset (Fig. 3F) for the 5 blocks of extinction training. There was a significant correlation between the amplitude of ERP responses recorded in MCN and vPAG for all available cases ($n = 6$ animals) for both CS+ onset and CS+ offset (onset, $p < 0.0001$; offset, $p = 0.033$; repeated-measures correlation).

Taken together these ERP data therefore suggest that population activity in MCN and vPAG broadly parallel the changes that occur in vPAG single unit peak activity at onset and offset of the CS+ during extinction of a fear conditioned response.

UOB Confidential

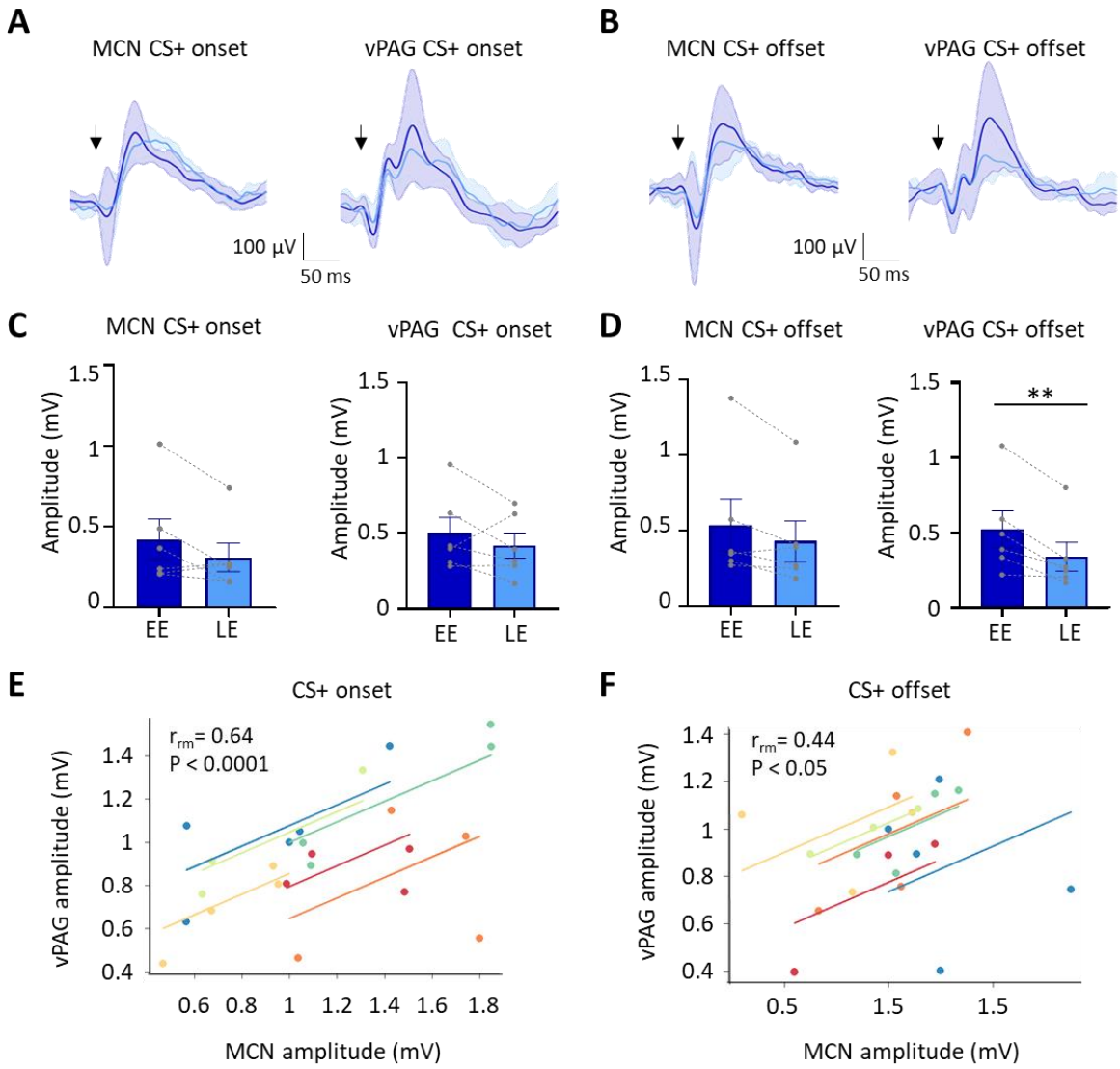

Figure 3. Auditory event related field potentials (ERPs) recorded simultaneously in the MCN and vPAG during extinction. A) Group average ERPs recorded at CS+ onset in the MCN and vPAG in control animals (n = 6 rats), arrows indicate time of tone onset; each waveform shows mean ± SEM; dark blue, average ERP during EE, light blue, average ERP during LE. B) Same as A but ERPs recorded simultaneously at CS+ offset (n = 6 rats). C) Plots showing mean peak to peak amplitude of ERPs recorded at CS+ onset in EE versus LE; left panel MCN, right panel vPAG (n = 6 rats, means ± SEM). Pairs of data points connected with dashed lines show the change in mean amplitude over extinction training for individual animals. D) Same as C but for CS+ offset (n = 6 rats, Paired t-test, ** $p < 0.01$). E) Repeated-measures correlation (r_{rm}) for ERPs at CS+ onset (n = 6 rats) comparing the amplitude of ERPs recorded simultaneously in MCN and vPAG. Each colour represents data and line of best fit for an individual animal. F) Same as E but for CS+ offset (n=6 rats).

The effect of temporary MCN inactivation on vPAG activity during fear consolidation

In 8 additional animals a delay conditioning paradigm was used (see Fig. 1A, 4 rats with bilateral cannulae in MCN and unilateral tetrodes in PAG, and 4 rats with bilateral cannulae only in MCN; see

UOB Confidential

Supplementary Fig 1. F,G), and muscimol was infused into the MCN to reversibly block cerebellar output during consolidation of the fear associative memory prior to extinction training (termed 'muscimol' in extinction sessions, Figs. 2, 4, 5; See also Supplementary Fig. 5). After a delay of 48hrs, to ensure complete washout of the drug, the animals were exposed to the unreinforced CS+ in extinction training. There was no significant difference between the overall firing rates across habituation, acquisition, and extinction training (Supplementary Fig. 2D, p = 0.079, one-way ANOVA).

In the 4 muscimol animals with tetrodes, a total of 14 type 1 vPAG units were recorded from 3 animals during extinction. Units were recorded from the fourth animal but were not type 1 responses so were not analysed further. Similar to the control results described above, the majority (71%, 10/14 units) of available type 1 onset units (Fig. 2C) showed a reduction in responsiveness during extinction training as measured by mean change in integrated area of response (Fig. 2D, on average the integrated area of response was 77.8 % smaller between EE and LE, p = 0.002, paired t-test). In keeping with the findings from control animals, no significant difference was found for mean peak z-score (Fig. 2E, peak 0.7% smaller between EE and LE, p = 0.971, paired t-test). There was also no statistically significant difference between control and muscimol animals for CS+ onset responses in EE or LE for either measure of response (Fig. 2D,E, mean integrated area in EE, p = 0.689, unpaired t-test; mean integrated area in LE, p = 0.351, unpaired t-test; mean peak z-score in EE, p = 0.919, unpaired t-test; mean peak z-score in LE, p = 0.654, unpaired t-test,), nor was there a difference in overall firing rates during extinction training (control vs muscimol, p = 0.685, unpaired t-test; Supplementary Fig. 2 C,D).

By comparison to controls (Fig. 2F, n = 23 units) inspection of Figure 2G (n = 10 units) shows that there was, however, a significant difference in muscimol experiments during EE in the average pattern of response of vPAG units at CS+ offset. The mean integrated area of response in muscimol experiments increased by 58.5 % by comparison to control (Fig. 2H, p = 0.002, unpaired t-test). There was also a reduction in mean peak z-score at EE (Fig. 2G, muscimol mean peak was 60 % of control) but this was not statistically significant (Fig. 2I, p = 0.515, unpaired t-test). In LE, the mean integrated area of response was also significantly different. On average, muscimol experiments had a significantly increased area of response than control animals (41.6 % larger, Fig. 2H, p = 0.014, unpaired t-test). Similar to CS+ onset, the mean peak z-score in LE was not significantly different between muscimol and control experiments (Fig. 2I, p = 0.32, unpaired t-test).

To investigate further the pattern of neural response between muscimol and control animals, we plotted for each unit the number of significant peaks of activity in the first 500 ms following CS+ onset and CS+ offset (see Methods for details). After CS+ onset, there was no significant difference in total number of peaks between muscimol and control animals (Fig. 4A; EE, p = 0.125; LE, p = 0.519; unpaired

UOB Confidential

t-test) nor latency to peak (Fig. 4B; p = 0.645, Chi-square), with both groups having about 85 % of peaks occurring in the 200 ms immediately following CS+ onset.

By contrast, following CS+ offset both the number (Fig. 4C; p < 0.0001, unpaired t-test) and latency (Fig. 4D; p = 0.01, Chi-square) of peaks significantly increased during EE in muscimol animals. In control animals 82 % of peaks occurred in the 200 ms immediately following the CS+ offset, while only 20 % of muscimol animals had peaks during the same time period.

Taken all together these data therefore suggest that during extinction training the pattern of response of vPAG units at CS+ onset is mainly unaffected by pharmacological block of MCN during consolidation, but the temporally precise activity at CS+ offset is disrupted during EE and LE, providing additional evidence that the two responses are independent of one another.

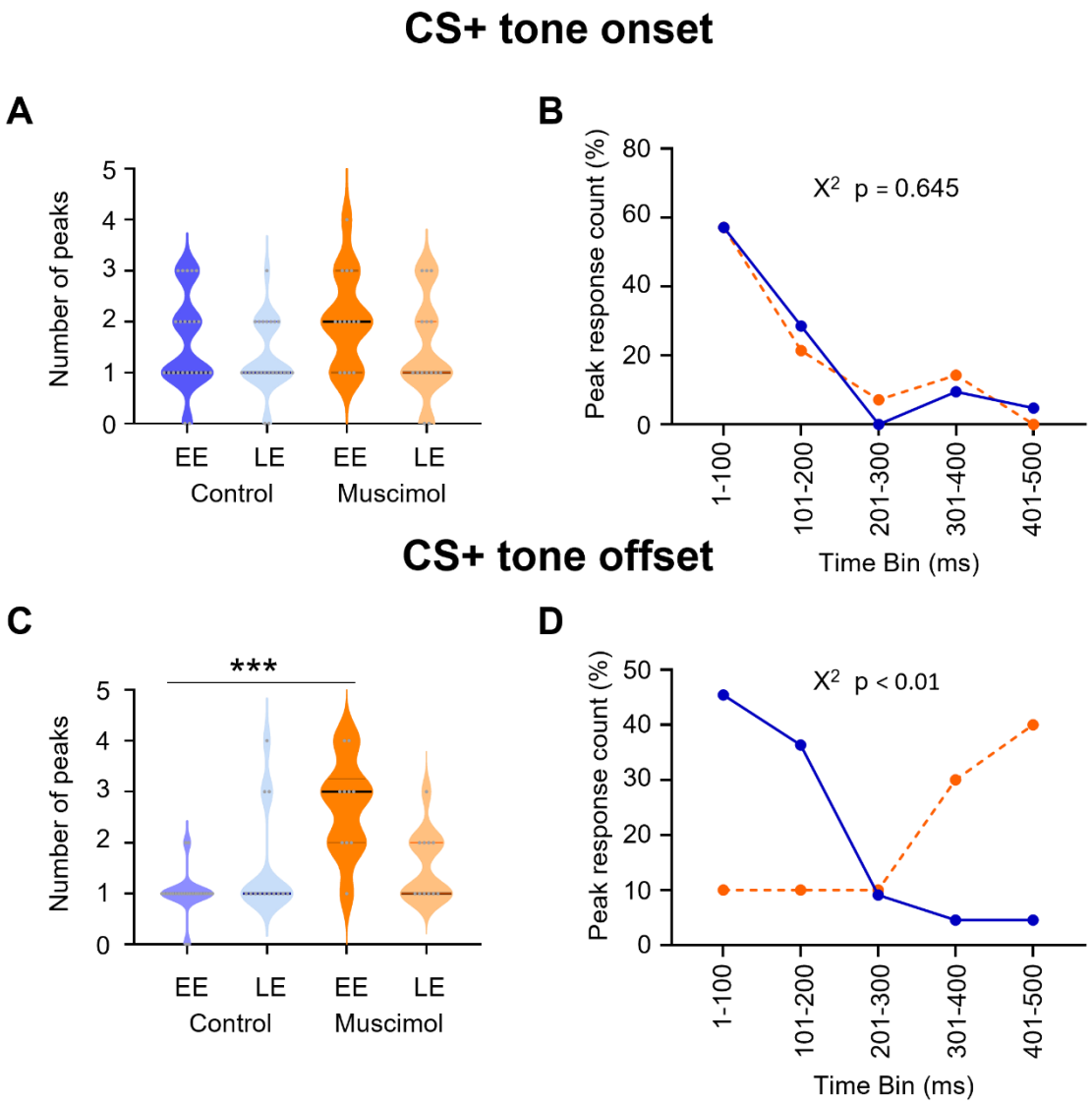

Figure 4. Effect of MCN inactivation during consolidation on the timing of vPAG type 1 onset and offset responses during extinction. A) Violin plots showing the number of significant peaks of activity (≥ 2SD from

UOB Confidential

baseline) that occur in the initial 500 ms following CS+ onset for EE and LE in control rats (blue, n=18 units) and muscimol rats (orange, n = 10 units). B) Proportion of peak responses as a function of time after CS+ onset. For each unit the 100 ms time bin in which the maximum peak response in the first 500ms occurred was expressed as a percentage of total count. Control (blue); Muscimol (orange). Chi squared test, $p > 0.05$. C) Same as A but for CS+ offset. *** $p < 0.001$, unpaired t-test. Control (blue, n = 19); Muscimol (orange, n = 10). D) Same as B but for CS+ offset. Chi squared test, $p < 0.01$.

The effect of temporary MCN inactivation during fear consolidation on behaviour

(i) Effects on freezing behaviour

To assess whether muscimol infusions into the MCN during consolidation had an effect on subsequent expression of fear-related freezing behaviour, different measures were taken during extinction training: % freezing during presentation of the CS+ and intertone interval (ITI), extinction rate during the CS+ and ITI, and the duration of freezing and movement epochs.

During presentation of the CS+, both control and muscimol animals showed extinction of the conditioned freezing response between EE vs LE (Fig. 5A; Control, EE freezing = 76.7 ± 4.1 % vs LE freezing = 32.6 ± 9.04 %, $p < 0.001$; Muscimol, EE freezing = 64.6 ± 4.4 % vs LE freezing = 23.7 ± 12.4 %, $p = 0.035$, paired t-tests. For trial-by-trial variation see Supplementary Fig. 6A). No significant differences were detected between control and muscimol animals in the percentage of time freezing during EE or LE (Fig. 5A; EE, $p = 0.098$; LE, $p = 0.579$, unpaired t-test), nor was there a difference detected in rate of extinction of freezing (Supplementary Fig.6; Control, -1.7 ± 2.0; Muscimol, -2.5 ± 0.6; $p = 0.473$, unpaired t-test). In terms of freezing behaviour during the ITI, both control and muscimol animals showed extinction learning similar to that found during presentation of the CS+ (Fig. 5B; EE vs LE: control, $p = 0.0003$, muscimol, $p = 0.014$, paired t-tests. For trial-by-trial variation see Supplementary Fig. 6B). There were no significant difference in muscimol animals by comparison to controls for either EE or LE (Fig. 5D; EE, $p = 0.21$. LE, $p = 0.929$, unpaired t-tests). Nor was there a significant difference in the rate of extinction between groups (Supplementary Fig. 6B; $p = 0.918$, unpaired t-test).

For baseline behaviour (see Methods) monitored just before extinction training there was no difference in the duration of freezing or movement epochs between control and muscimol animals (freezing duration for control 3.1(1.6, 6.5) s Med ± IQR and muscimol 4.5(3.6, 14.7) s Med ± IQR. $p = 0.195$, Mann-Whitney test. Movement duration for control 7.3(3.5,14.8) s Med ± IQR and muscimol 7.7(1.7, 27.12) s Med ± IQR. $p = 0.877$, Mann-Whitney test.). However, upon presentation of the CS+, there was a significant increase in the duration of freezing epochs in muscimol compared with control animals in both EE and LE (Fig. 5C; EE: Control 9.2(2.8, 14.7) s Med ± IQR, muscimol 26.45(14.5, 82.2) s Med ± IQR, $p = 0.014$, Mann-Whitney test. LE: control 3.4(2.3, 7.0) s Med ± IQR, muscimol 9.1(5.6,

UOB Confidential

23.5) s Med ± IQR, p = 0.026, Man-Whitney). There was also a significant increase in movement epochs in EE in muscimol by comparison to control animals, but there was no significant difference in LE (Fig. 5D; EE: Control 1.6(1.4, 2.0) s Med ± IQR, muscimol 4.09(2.4, 6.8) s Med ± IQR, p = 0.0028, Mann-Whitney test. LE: control 4(2.1, 11.0) s Med ± IQR, muscimol 8.5(3.0, 16.02) s Med ± IQR, p = 0.360, Man-Whitney).

As might be expected during extinction training, the duration of freezing epochs significantly decreased in both control and muscimol animals from EE to LE (Fig. 5C, Control, p = 0.039; muscimol, p = 0.008. Wilcoxon test) and there was a corresponding increase in the duration of movement epochs from EE to LE. However, the latter difference was statistically significant for controls (Fig. 5D; p = 0.033, Wilcoxon test) but not for muscimol treated animals (p = 0.250, Wilcoxon test). For individual measures of both freezing and movement duration see Supplementary Fig. 6C. Taken altogether these results therefore indicate that blocking MCN activity during consolidation does not alter the overall proportion of time spent freezing during subsequent extinction training, but does increase the duration of individual freezing bouts i.e., freezing bouts are longer but fewer in number as there are also longer bouts of movement.

To investigate the extent to which changes in unit activity correlate with fear behaviour during extinction training, the percentage of time spent freezing was compared to the average integrated area of unit responses after CS+ onset and also for the ITI following CS+ offset. Consistent with previous reports (Ozawa et al., 2017; Wright & McDannald, 2019), at CS+ onset there was a significant positive correlation in both control and muscimol groups between unit response and percentage time spent freezing for individual animals (Fig. 5E; Control, n = 7 rats, p = 0.048; Muscimol, n = 3, p = 0.038, repeated measures correlation). A significant positive correlation was also present between unit response at CS+ offset and percentage time spent freezing during ITI for both control and muscimol animals (Fig. 5F; Control, n = 7, p = 0.002; Muscimol, n = 3, p = 0.008, repeated measures correlation).

To investigate whether the extent of change in freezing behaviour and unit response during extinction training were related, a comparison was made between the absolute change in freezing for each animal with the mean absolute change in unit response. No significant relationship was found between freezing and unit response area at CS+ onset, nor for freezing during the ITI and unit response area at CS+ offset (Supplementary Fig. 6 C, D). Taken together these results therefore suggest that the magnitude of vPAG unit responses at both onset and offset of a conditioned tone reflect general fear state within an individual animal, but do not predict which individuals will have a stronger freezing response overall.

UOB Confidential

(ii) Effects on other defence-related behaviour

To investigate whether MCN inactivation during consolidation had an effect on other defence-related behaviours, rearing activity and ultrasonic vocalisations (USVs) were monitored during presentation of the CS+ and ITI during extinction training. However, by comparison to controls, no statistically significant effects were observed in either type of behaviour in muscimol animals (Supplementary Fig. 7E- H).

UOB Confidential

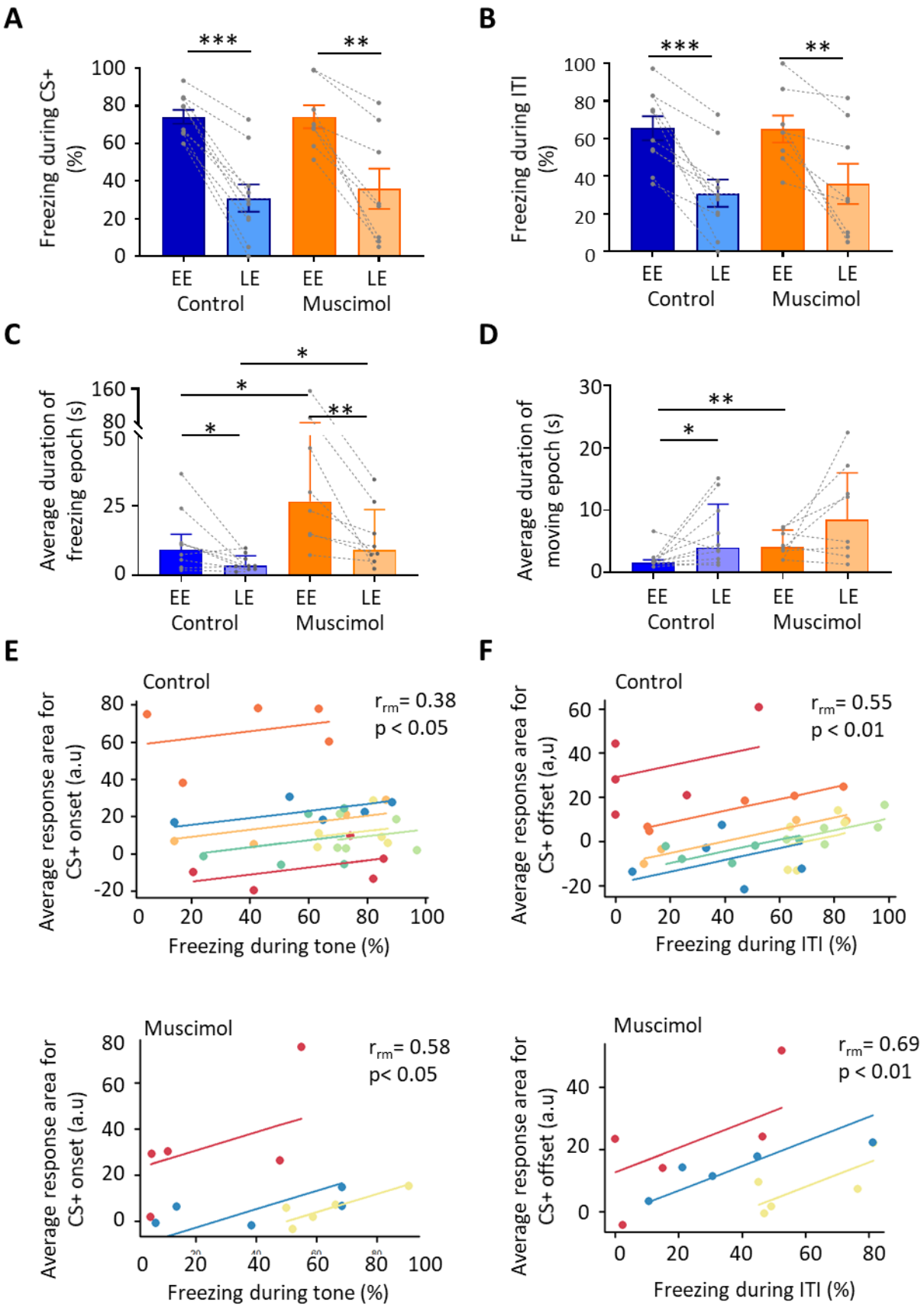

Figure 5. Freezing activity during extinction for control and muscimol animals. A) The percentage of total time the conditioned tone (CS+) was presented during EE and LE that freezing epochs occurred in control (n = 10 rats)

UOB Confidential

versus muscimol (n = 8 rats). Pairs of data points connected with dashed lines show the change in mean percentage freezing per animal over extinction training. Bars show group Med ± IQR. *** $p < 0.001$; ** $p < 0.01$. B) Same as A but for inter tone interval (ITI) . C) Same as A but for the average duration of time that animals displayed freezing behaviour after the CS+. Bars show group means ± SEM. Paired t test. ** $p < 0.01$, * $p < 0.05$. D) Same as C but for average duration of moving epochs. E) Repeated-measures correlation (r_{rm}) for control (upper panel, n = 7 rats) and muscimol (lower panel, n = 3 rats), comparing the integrated response area of units (arbitrary units, a.u) at CS+ onset as a function of percentage of time freezing during presentation of the CS+. Each colour represents data and line of best fit for an individual animal. F) Same as E but unit activity at CS+ offset in relation to time freezing during ITI.

Modulation of direct MCN to vPAG projection during fear acquisition and early consolidation

Given that during extinction training: (i) population activity in MCN resembles changes in vPAG population and unit activity; and (ii) the finding that global inactivation of MCN in rats can disrupt encoding in vPAG, it was of interest to determine whether the behavioural effects described above were dependent on a direct projection between the two brain structures. As a first step, a direct anatomical connection was investigated by injecting a fluorescently tagged anterograde virus into the MCN (n= 7 rats, Supplementary Fig. 8). In every case terminal projections in the PAG were primarily localised to its ventrolateral region on the contralateral side.

To investigate the function of this direct MCN-PAG projection, a viral vector encoding DREADD hM4D(Gi) (n = 10, AAV-hSyn-hM4D(Gi)-mCherry, termed DREADD, see Methods) or a control virus (n = 9, pAAV-hSyn-EGFP) was injected bilaterally into the MCN. Terminal projections containing either virus were targeted in the PAG by implanted cannulae to deliver CNO (for histological reconstruction of cannulae loci see Supplementary Fig. 9A). Note that while in the majority of our cases the infusion was centred on ventrolateral PAG, in keeping with studies of this type we cannot exclude spread to neighbouring areas of the midbrain.

To estimate the population of neurons that were manipulated in our viral vector experiments, in four animals we injected a retrograde tracer into ventrolateral PAG and the DREADD virus into MCN, and counted the proportion of double labelled neurons in MCN (Supplementary Fig. 10A). Double labelled neurons in MCN represented on average 70% ± 10.2 and 28% ± 8.3 when expressed relative to the PAG and DREADD single labelled populations, respectively (Supplementary Fig. 10B,C). These results therefore suggest that MCN-PAG projection neurons were likely to be transfected with DREADD in our experiments.

To determine the effect of MCN-PAG pathway modulation on conditioned fear behaviours, CNO was infused 15 minutes (Stachniak et al., 2014; Jendryka et al., 2019) before acquisition training to alter MCN-PAG projections during acquisition and early consolidation (Fig. 6A). During acquisition there was no significant difference in the percentage of freezing between control versus DREADD animals

UOB Confidential

during CS-US paired presentations (Fig. 6B upper panel, two-way repeated measures ANOVA; Time, $F(4.45, 75.64) = 16.63$, $p < 0.0001$; Virus, $F(1, 17) = 0.0889$, $p = 0.769$) nor during the ITI (Fig. 6B lower panel, two-way repeated measures ANOVA; Time, $F(3.834, 65.19) = 17.82$, $p < 0.0001$; Virus, $F(1, 17) = 2.339$, $p = 0.144$). However, comparison of the mean total number of USVs per animal in DREADD versus control groups across all acquisition trials showed that during the ITI, there was a significant reduction in number of USVs (Fig. 6C lower panel, a decrease of 36 %, $p = 0.032$, Mann Whitney test). This difference was not apparent during CS-US presentations (Fig. 6C upper panel, $p = 0.310$, Mann Whitney test).

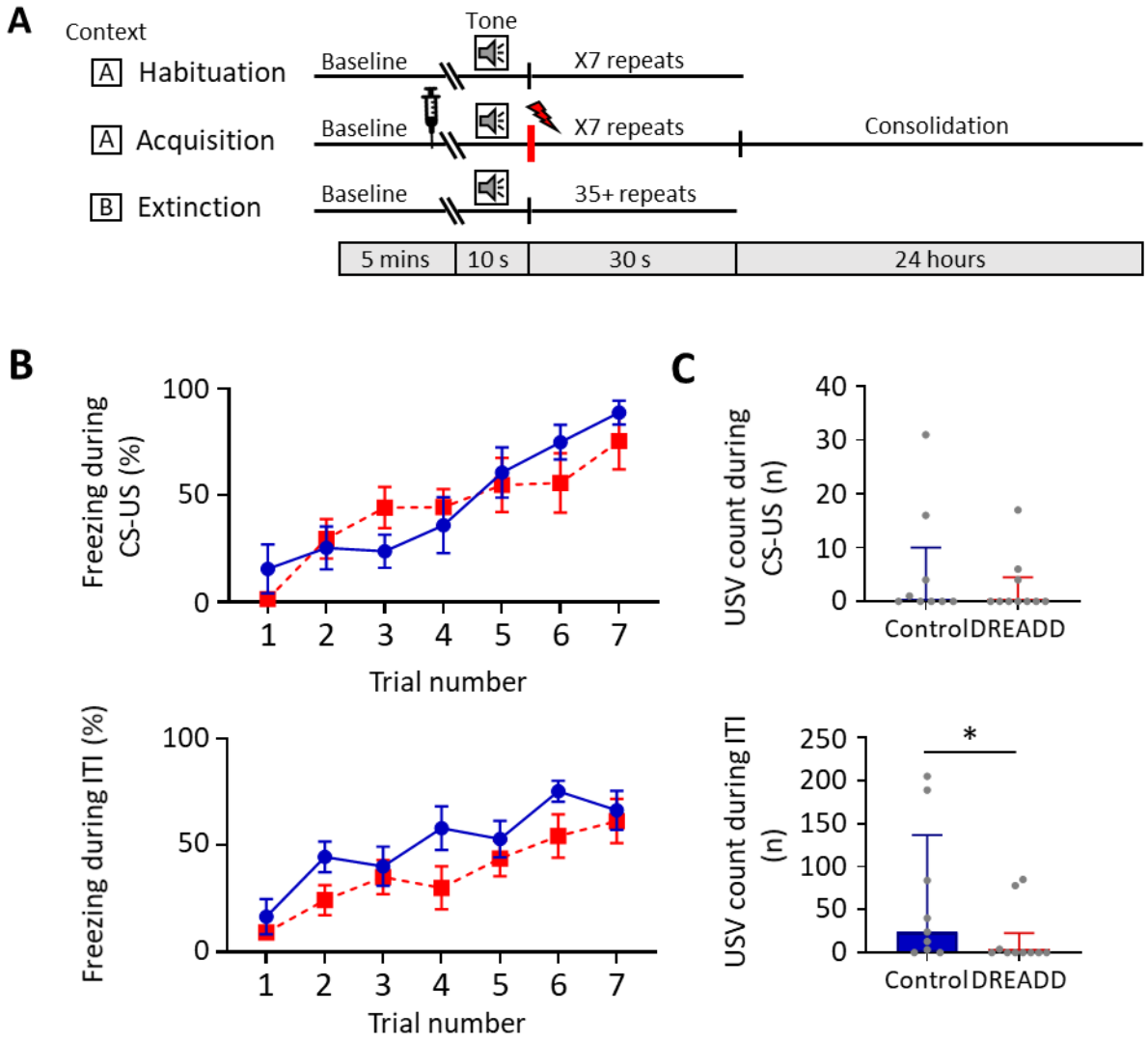

Figure 6. MCN-vPAG pathway inhibition and effect on behaviour during acquisition. A) Schematic timeline representing the fear conditioning protocol for the DREADDs experiment. B) The effect of CNO delivery into the vPAG during acquisition on freezing behaviour measured during presentation of the paired CS-US (upper plot), and the ITI (lower plot). Blue plot, control animals (n = 9 rats); red plot DREADD (hM4D(Gi)) animals, n = 10 rats); data points mean ± SEM. C) The number of ultrasonic vocalizations (USVs) recorded in control versus DREADD animals during CS-US presentation (upper panel) and during the ITI (lower panel); Bars show median ± IQR. Mann Whitney, one tailed test, * $p < 0.05$.

UOB Confidential

During extinction training, control and DREADD animals showed similar levels of freezing during presentation of the CS+ (Fig. 7A, EE $p = 0.645$, LE $p = 0.362$, unpaired t-test) and the ITI (Fig. 7B, EE $p = 0.501$, LE $p = 0.422$, unpaired t-test); for trial by trial variation see Supplementary Fig. 11A,B. Both groups also showed similar levels of extinction learning during CS+ (control, $p = 0.010$; DREADD, $p < 0.0001$, paired t-test) and the ITI (control, $p = 0.0042$; DREADD, $p < 0.0001$, paired t-tests). However, the rate of extinction during the CS+ was significantly slower in DREADD animals (Fig. 7C, $p = 0.042$, unpaired t-test), but not during the inter-CS+ interval (Fig. 7D; $p = 0.229$, unpaired t-test). The latter finding suggests the effect is not a general disruption of the expression of freezing behaviour.

With regard to rearing behaviour no differences were found between control and DREADD animals both within early and late extinction (Fig. 7E,F; EE CS+, $p = 0.305$; LE ITI, $p = 0.903$; LE CS+, $p = 0.273$; LE inter-CS+, $p = 0.786$, unpaired t-test), nor across all extinction training (Fig. 7E,F; EE vs LE; control CS+, $p = 0.556$, control ITI, $p = 0.269$; DREADD, CS+ $p = 0.244$; DREADD, ITI, $p = 0.111$, paired t-test,). Similarly, there was also no significant difference in the total number of USVs per animal in DREADD versus control groups across all extinction training (Fig. 7G,H; CS+, $p = 0.844$; ITI, $p = 0.849$, Mann Whitney tests; trial by trial variation see Supplementary Fig. 11C,D).

UOB Confidential

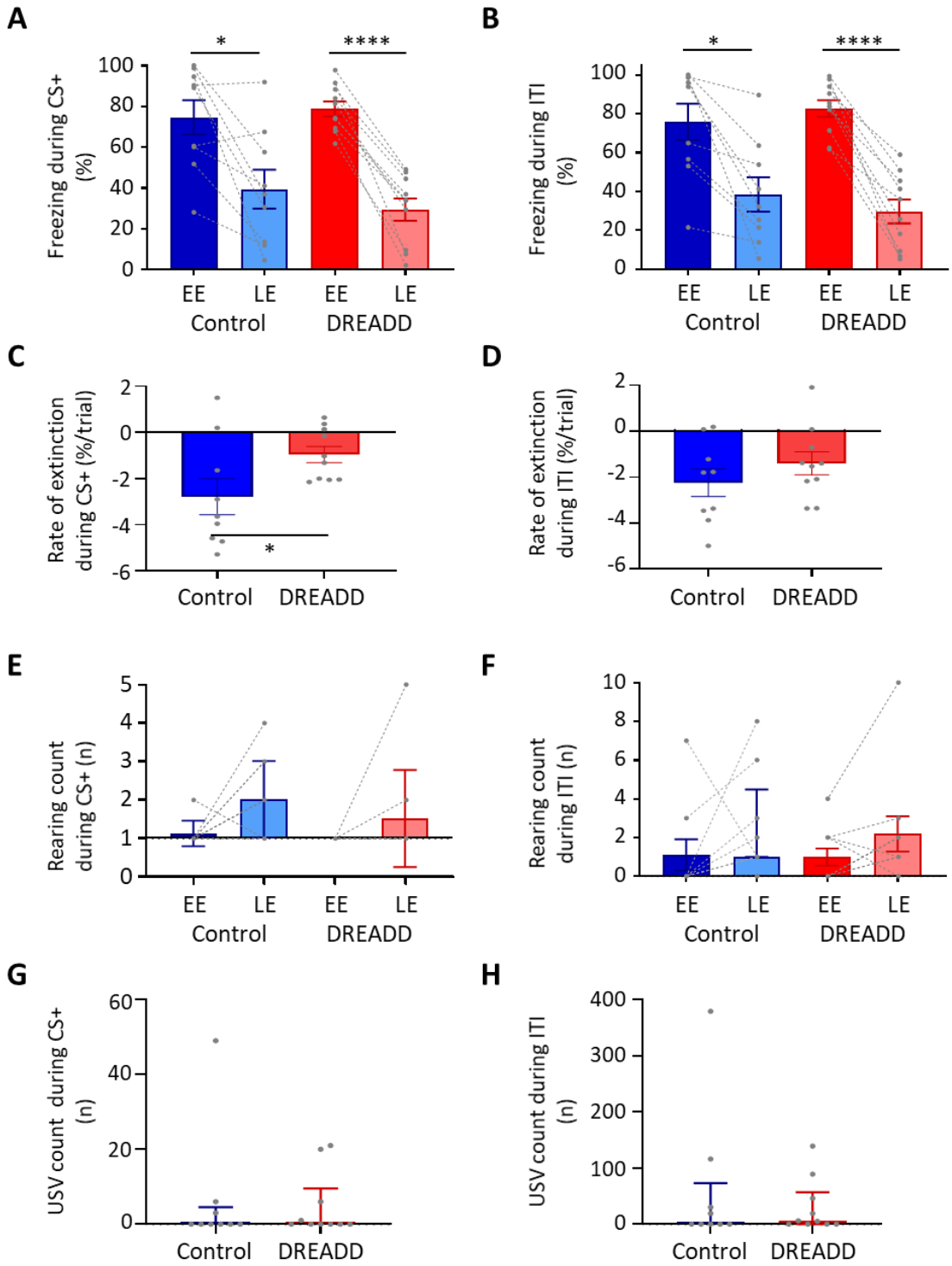

Figure 7. MCN-vPAG pathway inhibition effect on behaviour during extinction. A) The percentage of total time the CS+ was presented thatanimals displayed freezing behaviour during EE (trial 1-14) or LE (trial 21-35) in control (n = 9 rats) versus DREADD (hM4D(Gi), n = 10 rats). Pairs of data points connected with dashed lines show the change in mean percentage freezing per animal over extinction training. Bars show group means ± SEM. **** $p < 0.0001$, * $p < 0.05$. B) Same as A but for inter tone interval (ITI). C) Rate of extinction during presentation of the CS+ as measured by the change in percentage freezing over the first 21 CS+ presentations during extinction training in control (n = 9 rats) versus DREADD experiments (n = 10 rats). Individual data points show mean rate of change per animal. Bars show group means ± SEM. Unpaired t-test * $p < 0.05$. D) Same as C but for ITI. E) The total number of rears during presentation of the CS+ during EE and LE for control (n = 9 rats)

UOB Confidential

versus DREADD experiments (n = 10 rats). Pairs of data points connected with dashed lines show change in mean number of rears per animal over extinction training. Bars show group median and IQR. F) Same as E but for ITI. G) Total number of ultrasonic vocalisations (USVs) during presentation of the CS+ in extinction training in control (n = 9 rats) versus DREADD experiments (n = 10 rats). Individual data points show mean count per animal. Bars show group median and IQR. H) Same as G but total number of USVs recorded during ITI.

Control experiments for MCN-PAG intervention

To test for potential changes in anxiety and motor behaviour induced by modulation of the MCN-PAG pathway, the same DREADD and control animals studied in the fear conditioning experiments (n = 18 rats) were also tested on the following tasks after CNO infusion into vPAG: elevated plus maze, open field and beam walking. By comparison to controls, no statistically significant difference was found in any of these behaviours (Supplementary Fig. 9) Thus, no evidence was obtained to suggest that targeted modulation of the MCN-PAG pathway causes a general deficit in motor behaviour, nor a change in anxiety levels. However, insufficient effect of the DREADD on the MCN-PAG pathway cannot be ruled out.

In all available animals (controls, n = 8; DREADD, n = 9) we therefore made an intraperitoneal injection of CNO in order to test for non-specific effects, including general action on MCN and its projections. Consistent with the muscimol experiments, in every DREADD case, the CNO produced ataxia, although this was generally less severe and shorter lasting (~1h) than was observed in the muscimol animals. Impairments in motor behaviour were assessed by testing the animals on the beam walking task; DREADD animals were significantly slower than control animals at traversing the beam (Supplementary Fig. 9F, p = 0.006, unpaired t-test).

UOB Confidential

Discussion

We have shown that vPAG neurons (type 1 units) encode temporally precise information about both the onset and offset of a fear conditioned auditory stimulus and that these two neuronal signals may be generated by independent mechanisms. This is because during extinction: i) some vPAG units only respond to CS+ onset or only to CS+ offset; ii) unit onset and offset responses exhibited different characteristics during extinction training; iii) MCN inactivation during consolidation disrupted the vPAG pattern of unit activity at CS+ offset but not onset; (iv) the latency of the event related potential (ERP) at CS+ onset was significantly shorter than the ERP recorded at CS+ offset; and (vi) the ERP recorded at CS+ onset remained similar in amplitude over extinction training while the ERP at CS+ offset showed a significant reduction.

Importantly, vPAG units displayed little or no response to an auditory tone during habituation but displayed robust activity at tone onset and/or offset when the same tone was classically conditioned. This provides evidence that the responses were related to the associative conditioning rather than the sensory stimulus. Moreover, disruption of the temporal precision of the conditioned tone offset neural response following MCN inactivation suggests a role of the cerebellum in the timing, but not the generation, of the vPAG offset response.

More generally, our study applied novel approaches to address fundamental questions about the role of cerebellar-PAG interactions in survival behaviour. As such, consideration of the methods used is critical to the interpretation of the data and is included in the Methods section.

Comparison to previous behavioural studies

Previous inactivation studies in rats using TTX have indicated that the cerebellar vermal cortex is involved in the consolidation of associatively conditioned cue and context dependent fear memories (Sacchetti et al., 2002). This suggests that the vermal compartment of the cerebellum is involved in various aspects of fear learning. The finding in the present study that inactivation of a major output of the vermal compartment, MCN, leads to deficits in both USVs and freezing behaviour, strongly supports this multiplicity of function.

The present results are also consistent with Frontera et al., (2020) who found in mice that inactivation of the MCN-PAG pathway during acquisition but not consolidation reduced the subsequent rate of extinction of conditioned freezing behaviour during retrieval. The present experiments in rats found DREADD-induced modulation of the MCN-PAG pathway during acquisition slowed subsequent

UOB Confidential

extinction rate, while muscimol inactivation during consolidation had no detectable effect on freezing behaviour (suggesting comparability across species). The novel finding reported here shows that muscimol inactivation during consolidation increases the duration of both freezing and movement bouts during retrieval of the conditioned response. This suggests that during consolidation the influence of MCN on survival circuits has an effect on the subsequent temporal profile of behavioural responses during retrieval but not the strength of the fear-related memory. We also show that modulation of the MCN-PAG pathway during acquisition reduces the expression of fear-related USVs at this time. Taken all together this raises the possibility that the MCN regulates different aspects of survival behaviour depending on the stage of fear conditioning.

Comparison to previous electrophysiological studies

In regard to our electrophysiological findings, similar responses to CS+ onset in vPAG have been reported previously by ourselves (Watson et al., 2016) and others (Ozawa et al., 2017; Wright & McDannald, 2019), but to our knowledge no equivalent response precisely time locked to CS+ offset has been described. This may be due to differences in the characteristics of the auditory cue used for conditioning (e.g., duration, intensity and rise-fall time of the tone: Takahashi et al., 2004; Qin et al., 2007; Scholl et al., 2010; Harris et al., 2017; Sołyga et al., 2019), but also because detection of such responses depends on the temporal resolution used for the analysis. For example, Watson et al., (2016) used, as is the case in many other electrophysiological studies, a 1 sec bin width to visualize the patterns of vPAG activity during CS+ presentation. Because offset responses are brief, temporally precise, events we found that a 40 ms bin width was needed to reliably capture them.

Fear conditioned CS+ onset responses in vPAG are thought to be generated, at least in part, as a result of preceding activity in the amygdala (Tovote et al., 2016;) and may encode multiple aspects of fear processing, including maintenance of fear memory after extinction (Watson et al., 2016), prediction error coding (Ozawa et al. 2017), the transmission of aversive teaching signals to the amygdala (Johansen et al., 2010) and threat probability (Wright and McDannald, 2019). vPAG activity has also been correlated to the onset of freezing behaviour (Tovote et al., 2016; Watson et al., 2016) indicating that there may be several distinct neuronal populations in the PAG that are responsive to conditioned stimulus onset. Our results for CS+ onset responses are consistent with Watson et al., (2016), as we show the phasic increase in neural activity was dependent on associative conditioning, and type 1 onset responses were generally smaller in late extinction by comparison to early extinction (i.e. were extinction sensitive) and therefore may contribute to the neural plasticity associated with extinction learning.

UOB Confidential

In terms of previous reports of CS+ offset responses in vPAG, Wright and McDannald (2019) identified a distinct population of units in an auditory fear discrimination task they termed ramping units. These units were related to threat probability and also to fear output as determined by freezing behaviour. Ramping units progressively increase activity over the duration of the auditory cue presentation, reaching a peak around sound offset and ramping down in activity thereafter. This pattern differs markedly from our type 1 offset units whose phasic activity was precisely coupled to CS+ offset. Indeed, we found no evidence of ramping type activity in our sample of vPAG units. This is perhaps unsurprising because the experimental paradigm of Wright and McDannald (2019) differed from ours in a number of important ways. In particular, they used a trace fear conditioning protocol where the aversive footshock was paired in each session with the auditory cue with a varying probability of occurrence. The closest comparison with our results is between our acquisition sessions and their trials when the probability of a footshock was 100% (their Fig. 1). In our experiments, immediately after the footshock (the stimulus artefact prevented data recording during the unconditioned stimulus) we observed an increase and a subsequent progressive reduction in spike activity that resembled the change in firing after peak in their ramping units (our Fig. 1C).

An unanswered question concerns the origin of CS+ offset responses in vPAG. We estimate that they occur approximately 30 ms after the end of the CS+ tone. Such a delay provides ample opportunity for many possible pathways to generate them. Detecting the offset (and onset) of sensory events is a fundamental requirement of sensory processing by the CNS. Given the importance in the present experiments of the auditory system in the initial processing of the tone signals used for fear conditioning, one possibility is a route from the auditory cortex to the PAG. Both onset and offset responses have been reported in the auditory cortex elicited by tones and other sounds in a range of species (Qin et al., 2007; Tian et al., 2013; Liu et al., 2019). Also, changes in activity in the auditory association cortex during fear conditioning have been shown to precede the expected time of the unconditioned stimulus (Quirk et al., 1997). In principle, such activity occurs sufficiently in advance of our CS+ offset responses to be driving them. However, pathways from the auditory system to the PAG target its dorsolateral and lateral sectors and are associated with flight behaviour (e.g. Wang *et al.*, 2019), so presumably some other pathway is responsible. For example, the medial prefrontal cortex and the bed nucleus of stria terminalis have extensive projections to the PAG (Holstege et al., 1985; An et al., 1998), and after fear conditioning both show sustained changes in activity during presentation of the CS+ (Haufler et al., 2013; Gilmartin et al., 2014).

A further important question relates to what information CS+ offset responses encode. Learning theory proposes that Pavlovian fear conditioning is instructed by an error signal that encodes the difference between actual and expected intensity of the US (Rescorla & Wagner, 1972; Mcnally et al.,

UOB Confidential

2011). The vPAG is generally considered to provide the teaching signal that encodes aversive prediction error to regulate synaptic plasticity in the amygdala and prefrontal cortex during fear extinction learning (Johansen et al., 2010; Mcnally et al., 2011; Roy et al., 2014; Walker et al., 2019; Frontera et al., 2020). According to the Rescorla-Wagner learning model this teaching signal is modulated by expectation of the US – during retrieval of a fear conditioned association the unreinforced CS+ produces a negative prediction error signal because the US has not occurred as expected. The reliability of this prediction is reduced with successive presentations of the unreinforced CS+. If fear extinction is instructed by this error signal, then neurons encoding prediction errors would be expected to progressively decrease their CS+ induced firing rate upon repeated omission of the expected US (McNally et al., 2011). In the present study the gradual reduction in CS+ type 1 offset responses in vPAG during extinction training are entirely consistent with this proposition. However, in our trace conditioning experiment the failure of CS+ offset responses to follow the timing of the expected US would seem to argue against this, although the 1 sec time interval we used may have been too short for rats to discriminate. Another possibility is the CS+ offset response is signalling saliency of the tone, but this can also be thought of as a component of generating prediction error. Clearly further studies are required, but the current findings open new avenues for investigating the role of vPAG in encoding fear memory.

We also show that inactivation of the cerebellar output nucleus MCN during consolidation disrupts but does not abolish CS+ type 1 offset responses in vPAG upon retrieval of the fear memory. This is line with MCN modulating vPAG activity (Vaaga et al., 2020), and advances understanding by raising the possibility that the vermal compartment of the cerebellum is involved in the timing of the memory trace, but not the origin of CS+ offset signals in vPAG. Consistent with this suggestion is the finding that in mice, phasic optogenetic stimulation of the MCN-vPAG pathway during CS+ offset significantly enhanced extinction learning, while tonic activation using chemogenetics had the opposite effect (Frontera et al., 2020), suggesting that the temporal pattern of activation of vPAG neurons by MCN determines the effect on extinction learning.

Functional significance

A role of MCN in temporal patterning is in good agreement with the timing hypothesis of cerebellar function (Ivry, 1997; Cheron et al., 2016; D'Angelo, 2018). This hypothesis proposes that the cerebellum not only regulates the timing of movement to enable coordinated behaviour and motor learning, but that this temporal regulation extends to other functions of the CNS, including perceptual tasks that require the precise timing of salient events (Spencer et al., 2013). The present study extends this concept to the encoding of fear memory by vPAG. Our findings suggest that the

UOB Confidential

cerebellum is important for the regulation of fear memory processes at multiple timescales: at the millisecond timescale to control the neural dynamic encoding of CS+ offset within vPAG, and at longer timescales (secs/hours/days) to regulate the duration of freezing and movement bouts during extinction, the rate of fear extinction, and the timing of expression of fear-related behaviours - MCN indirectly influences fear conditioned freezing behaviour during extinction training but more directly is also involved in the expression of USVs during acquisition. It is tempting to speculate that the influence of MCN on survival circuits during consolidation that lead to the temporally precise encoding of CS+ offset by vPAG during retrieval, also underlies the behavioural effects we observed during extinction, but this remains to be determined.

Cerebellar manipulations can affect emission of USVs (Fujita et al., 2008, 2012; Umeda et al., 2010; Fujita-Jimbo et al., 2014). Taken together with our USV results this raises the possibility that the MCN-vPAG pathway regulates the emission of USVs at a time when danger is greatest, perhaps as a warning signal to conspecifics. Our results also suggest that activity in the MCN-vPAG pathway during acquisition regulates the subsequent rate of fear extinction, consistent with a previous study in mice (Frontera et al., 2020). Outbred strains of rats have been shown to demonstrate different behavioural phenotypes during fear extinction (Ji et al., 2018) where a proportion of animals show faster rates of extinction than others. Interruption of MCN-vPAG interaction during acquisition or early consolidation may therefore contribute to an anxiety-like behavioural phenotype, with wider implications for possible neural mechanisms that underly psychiatric disorders such as PTSD.

In summary, MCN is part of a survival circuit network that regulates the precise temporal encoding of fear memory within vPAG and also regulates the expression of different survival behaviours depending on the phase of Pavlovian fear conditioning. Inactivation of MCN output during consolidation increases the duration of freezing and movement epochs during extinction, while a direct pathway to the vPAG appears to be important in eliciting fear related USVs during acquisition, and the rate of expression of freezing during early extinction. The cerebellum through its interactions with the survival network might therefore be coordinating the most appropriate behavioural response at the most appropriate time.

Methods

Animals: All animal procedures were performed in accordance with the UK Animals (Scientific Procedures) Act of 1986 and were approved by the University of Bristol Animal Welfare and Ethical Review Body. A total of 47 adult male Sprague Dawley rats (280-400g; Harlan Laboratories) were used in this study. They were housed under normal environmental conditions in a normal 12 h dark/light

UOB Confidential

cycle and provided with food and water *ad libitum*. Animals were single housed after surgery to prevent damage to implants.

Surgical procedures for chronic implants:

Rats were anaesthetised initially with gaseous isoflurane, followed by intraperitoneal injections with ketamine and medetomidine (5 mg/100g of Narketan 10 and Domitor, Vetoquinol). Each animal was mounted in a stereotaxic frame with atraumatic ear bars and surgery was performed under aseptic conditions. Depth of anaesthesia was monitored regularly by testing corneal and paw withdrawal reflexes with supplementary doses of ketamine/medetomidine given as required. A midline scalp incision was made, and craniotomies were performed to gain access to the cerebellum and/or the PAG as required in each line of experiment. Microdrives and/or cannulae were implanted and/or viral injections were made as described below depending on the experiment. At the end of every surgery, the rat was administered the analgesic Metacam (Boehringer Ingelheim, 1 mg/Kg) and the medetomidine antidote Atipamezole (Antisedan, Vetoquinol 0.1mg I.P.). Animals were handled for 1 week prior to surgery and during recovery before any behavioural paradigms or electrophysiological recordings were undertaken.

Electrophysiological recordings and cannulae (n = 22 rats):

1). Dual microdrive experiments (n = 6 rats). Two in-house built microdrives, designed to slot closely next to each other, were positioned over craniotomies to allow tetrodes to be independently advanced into the right MCN (11.4 mm caudal from bregma, 1 mm lateral from midline, depth of 4mm) and contralateral vPAG (7.5 mm caudal from bregma, 1 mm lateral from midline, depth 4.8mm). The microdrives were attached to the skull with screws and dental acrylic cement. Each microdrive contained 3-4 tetrodes for local field potential (LFP) and single unit recording (0.0008-inch Tungsten wire 99.95 % CS 500 HML, insulated with VG Bond, 20 µm inner diameter, impedance 100-400 KΩ after gold plating; California Fine Wire). 2). Single microdrive experiments (n = 12 rats). These implants were the same as described above except only one microdrive was implanted to record single units from the vPAG. In 8 of these animals infusion cannulae were implanted bilaterally to target the MCN (4 with muscimol and 4 with saline) during delay conditioning experiments (details below). The remaining 4 animals were used in trace conditioning experiments. Single units were recorded from 3 of these animals.

Since similar electrophysiological data (see Supplementary Figs. 2, 3), were recorded from the PAG obtained from animals with a dual microdrive (PAG and MCN, tetrodes only controls) and those with a single microdrive (PAG, that received a saline infusion into MCN, saline controls) the results have

UOB Confidential

been pooled (collectively termed 'control'). There was no significant difference between the overall firing rates across habituation, acquisition and extinction training (Supplementary Fig. 2C, p = 0.649, one-way ANOVA). Thus, it seems reasonable to assume that single unit recording was stable over time and comparable between groups.

Muscimol infusions

Effects of the muscimol infusion on general motor co-ordination were carefully monitored. Immediately after the infusion all animals (n = 8 rats) displayed mild to moderate ataxia, providing a positive control that the muscimol was disrupting cerebellar activity. The severity of the ataxia gradually reduced over several hours and the animals were behaviourally normal after 24hrs.

Anatomical pathway tracing (n = 7 rats):

To anterogradely map direct connections between MCN and PAG, 100nl of an adeno associated viral (AAV1) vector expressing tdTomato under the CAG promoter was injected unilaterally into the MCN (11.4 mm caudal from bregma, 1 mm lateral from midline, depth of 4.5 mm). pAAV-CAG-tdTomato (codon diversified) was a gift from Edward Boyden (Addgene viral prep # 59462-AAV1; http://n2t.net/addgene:59462; RRID:Addgene 59462). Injections of the AAV were made following previously published methods (Hirschberg et al., 2017). In brief, the glass micropipette was connected to a 25 µl syringe (Hamilton, Bonaduz, Switzerland) via tubing filled with dyed mineral oil, and was then backfilled with virus using a syringe driver (AL-1000, World Precision Instruments). To monitor progress of the injection, movement of the oil-vector capillary interface was monitored. Injections were made at 200 nl/min and the pipette left in situ for 5 min prior to removal. Survival time 3 weeks prior to terminal perfusion and histology (see below).

DREADD surgery (n = 24 rats):

For the DREADD experiments *t*wo adeno associated viral (AAV) vectors were used: a control, pAAV-hSyn-EGFP (AAV5); and active DREADD, pAAV-hSyn-hM4D(Gi)-mCherry (AAV5) (both gifts from Bryan Roth, Addgene viral prep # 50465-AAV5 and # 50475-AAV5). Using the same techniques as outlined above, animals were injected bilaterally into MCN with 350 nl of either the control (n = 12) or the DREADD (n = 12). In the same surgery bilateral cannulae (26-gauge guide cannula, PlasticsOne) were also chronically implanted with tips (33 gauge internal) located just above the ventrolateral PAG (7.5 mm caudal from bregma, 0.8mm lateral from midline, at a depth of 5 mm).

Double tracing (n = 4 rats):

UOB Confidential

To assess the proportion of PAG projecting neurons transfected with the DREADD virus, 4 animals were injected with the DREADD virus in the MCN as described above and with a rAVV-CAG-GFP (AAVr) retrograde virus into ventrolateral PAG (7.5 mm caudal from bregma, 0.8 mm lateral from midline, at a depth of 5 mm). Survival time was 3 weeks prior to terminal perfusion and histology (see below).

Behavioural protocols:

Auditory cued fear conditioning (n = 46 rats). The delay conditioning paradigm was based on Watson et al. (2016, Fig1A). On day 0 all animals underwent a session of habituation to the Skinner box (context A, Med Associates Inc., St Albans, VT, USA) to act as a baseline for analysis prior to a session of acquisition in the same context (day 1). During acquisition, the conditioned stimulus (CS, 2KHz, 10sec tone) was paired 7x with an unconditioned stimulus (US, 0.5 s footshock, 0.75 mA) delivered at the end of the tone, except in four animals where the timing of the US was delayed 1sec after the CS (trace conditioning). In all animals this was followed by a single session of extinction training in a different context (context B), on either day 2 (tetrodes only animals) or day 3 (muscimol and saline control animals). During extinction, 7 tone presentations (trials) were repeated in 5 blocks. The first two blocks (trials 1-14) were defined as early extinction (EE), when the animal was exhibiting high levels of freezing, while the last two blocks (trials 21-35) were defined as late extinction (LE), when the animals exhibited low levels of freezing.

Balance beam (n= 18 rats). This test was used to assess general motor coordination and balance (Luong et al., 2011). Animals were trained for 3 consecutive days to cross a 160 cm long beam that ended on an enclosed safety platform (6 traversals of the beam per day). On each day, the beam was progressively thinner in width (6 cm, 4 cm and 2 cm). The 2 cm beam was then used for the test day. Baseline performance was recorded and then CNO (Clozapine N-oxide) was administered either i.p. or by intracranial infusion (for details see below). After an interval of 15 minutes the animal was re-tested on the beam. Beam balance performance was manually scored using Solomon Coder software (© 2019 by András Péter), measuring the time to cross the beam for the baseline and test trials.

Open field (n = 14 rats). This test was used to assess both general motor behaviour and anxiety levels. Animals were exposed for the first time to the circular arena on the test day (90 cm diameter, 51 cm height). They were placed at the perimeter of the arena and were allowed to explore for 10 minutes. Videos were recorded of exploratory behaviour for the whole session and DeepLabCut (Wei et al., 2018) was used to track animal behaviour. The total distance travelled, and time spent in two equivalent areas of the arena (centre and a periphery) were calculated.

UOB Confidential

Elevated plus maze (n = 18 rats). This test was used as an additional assessment of anxiety (Pellow et al., 1985). Animals were placed in a plus shaped maze, 1 m above the floor, with 2 open and 2 closed arms (10 cm wide and 50 cm length) and allowed to explore the maze for 5 minutes. Performance was manually scored using Solomon encoder software (© 2019 by András Péter) to calculate the percentage of total time spent in the open versus closed arms.

<u>*Data acquisition and analysis:*</u>

Electrophysiological recording. Multisite electrophysiological data were recorded using a Blackrock Microsystems (Utah, USA) data capture system synchronised with OptiTrak software. Neural data were sampled at 30 kHz and band pass filtered online between 300 Hz – 6 kHz.

Auditory cued fear conditioning. Video recording of animal behaviour during the fear conditioning paradigm was captured with an OptiTrak camera and software, allowing synchronisation with neural data. Fear-related freezing behaviour was manually scored using Solomon Coder software (© 2019 by András Péter). Freezing behaviour was identified as periods in which the animal had an absence of movement (except those associated with respiration and eye movements, Blanchard & Blanchard, 1969) while typically maintaining a crouching position. Percentage of time spent freezing was calculated for each trial during CS+ presentations and during inter tone intervals (ITI). The duration of freezing and movement epochs was also assessed for each animal during three different time periods: (i) baseline (the average of the last 5 freezing and the average of the last 5 moving epochs immediately before CS+ onset), (ii) EE (same as baseline but the 5 freezing and movement epochs following the first CS+ onset) and (ii) LE (same as baseline but the first 5 freezing and movement epochs following onset of CS+ presentation 22). To evaluate the extinction rate of freezing behaviour, the slope of the trendline of changes in freezing % over the initial 3 blocks of extinction training was calculated (trials 1-21, by trial 21, 50% of control animals reached extinction). Rearing activity was counted as the number of events in which the animal moved from the floor to standing upright on its rear limbs. The number of rearing events during CS+ presentations and ITIs was counted.

Ultrasonic vocalisation recordings. USVs emitted at 22 kHz were recorded using an ANL-940-1 Ultrasonic Microphone and Amplifier (Med Associates, Inc.) connected to the Blackrock Microsystems (Utah, USA). Although USVs were recorded as an aliased signal (the maximum sampling rate of the recording system was 30 kHz, while the optimal sampling rate was 44 kHz) we were able to identify USV events. For analysis, USVs were visualised using Spike7 software (Cambridge Electronic Design Limited) and individual USV emissions manually identified and the total number counted during each recording session.

UOB Confidential

Control behavioural tests: Beam balance, open field and elevated plus maze tests were recorded via standard webcams linked to OBS (Open Broadcaster Software; © 2012-2020).

Inactivation experiments (n = 12). In 8 animals muscimol (Sigma Aldrich, 0.3 ul, at a rate of 0.3 ul/min) (or saline; n = 4 animals) was infused via indwelling cannulae at a rate of 0.3 ul/min to target MCN. The infusion was made immediately after acquisition (i.e., during early consolidation). Extinction training was carried out 48 hours after the infusion (day 3).

DREADD experiments:

A total of 24 rats were randomly assigned to either a saline control (n = 12) or a DREADD experimental group (n = 12) and coded so the experimenter was blinded. A total of 9 controls and 10 DREADD animals were included in the analysis. The remainder (5 animals) were excluded because post mortem histology showed off-target cannulae placement.

Unblinding occurred once all procedures and analysis were completed. Six weeks after viral transfection (see above), animals were tested in the following behavioural paradigms: auditory cued fear conditioning, beam balance, open field and elevated plus maze. One animal was excluded from the study after the fear conditioning test because of poor health; a further 3 animals were excluded from the open field analysis because of technical problems with the video recording. In every animal a volume of 500nl of CNO (3 µM, Tocris) was infused at a rate of 0.5µl/min to target the PAG, 15 minutes prior to each behavioural test (infusion pump Harvard Apparatus, PHD 2000 Infusion). Since the effect of CNO is estimated to last 60-90 mins (Stachniak et al., 2014; Jendryka et al., 2019) this meant that during fear conditioning, the pathway under study was likely to be inhibited during both acquisition (which lasted about 10 mins) and also a subsequent period of early consolidation. To verify functional activity of hM4D(Gi) receptors in the CNS following MCN transfection with DREADD, CNO was injected i.p. (2.5 mg/Kg) 20 minutes before the beam balance test.

Histology:

At experimental end points all animals were deeply anaesthetized (Euthatal, 200 mg ml^{-1}, Merial Animal Health) and terminated by transcardial perfusion (4% paraformaldehyde in 0.1 M phosphate buffer) and the brains extracted. After post-fixation, the brains were cryoprotected in 30% sucrose solution. The cerebellum was cut sagittally and the midbrain including the PAG cut coronally, into sections of 40 or 60 µm thickness, respectively. To aid verification of electrode and cannula brain loci, sections were stained with cresyl violet. Because of the inherent limitation of localising the tracks of multiple tetrode implants in an awake animal we cannot exclude the possibility that some units

UOB Confidential

were located in other ventral parts of PAG. For this reason we use the term ventral PAG (vPAG, see also Watson et al 2016).

For visualisation of viral expression immunohistochemistry for anti-mCherry (1:2000, Anti-mCherry Polyclonal Antibody host rabbit, BioVision, with 5% normal horse serum (NHS); 1:1000, Alexafluor 594 donkey anti Rabbit IgG, Molecular probes) was performed. No signal amplification was required for the eGFP controls. Sections were visualised on an Axioskop 2 Plus microscope (Zeiss) and photomicrographs captured using AxioVision software, or with a widefield microscope (Leica DMI6000, with Leica DFC365FX camera and Leica LASX live cell imaging workstation software).

Neural data analysis:

Spike sorting. Offline spike sorting was carried out using MClust software in Matlab. Clustering was classified as single unit if L ratio < 0.35, ID > 15 and < 1 % of interspike intervals was > 2 ms (See Schmitzer-Torbert *et al.*, 2005). For an example tetrode recording and its isolated spikes see Supplementary Fig. 1A , B. The firing rate of individual units was taken from MClust and verified using NeuroExplorer.

Data analysis of single units:

For habituation, acquisition and extinction training sessions, peri event time histograms (PETHs, 40 ms time bins) of the activity of individual units were created in NeuroExplorer, with tone onset and offset as time zero. During acquisition, the footshock caused electrical interference so it was not possible to record unit activity during the 0.5 sec period of stimulus delivery. The following analysis was performed in MATLAB. In all experimental groups PETHs of unit activity to the unreinforced conditioned tone (CS+) during extinction training were constructed for individual units over all trials (1-35) and also separately for early extinction (EE, trials 1-14) and late extinction trials (LE, 21-35). PETHs were z-score normalised to a 5 second baseline recording of unit activity immediately before CS+ onset and data grouped according to response type and averaged. A significant response was defined as 1 or more consecutive 40 ms time bins where the z-score was ± 2 SD from baseline mean in the first 500ms following the tone. The area of the response was calculated as the trapezoidal numerical integration of the first 1 second after tone onset or offset (arbitary units). Peak z-score was measured for each unit at the time where the average peak response occurred. Total peak number was calculated as the sum of all (non-consecutive) 40ms time bins where the z-score was ± 2 SD from baseline mean within the first 500ms after tone onset. The first 500 ms period after tone onset was also divided into 100 ms time bins and the proportion of units with maximal peak response within

UOB Confidential

each bin expressed as a percentage of total number of maximal peaks. Maximal peak per unit was identified as the response with the largest increase relative to baseline mean.

Data analysis of Local field potential. Local field potential (LFP) data were averaged in relation to tone onset and offset using MATLAB (n = 14 trials per mean of each animal). The tetrode recording site yielding the largest mean amplitude peak to trough response was identified in each animal and used to calculate group average data of peak amplitude of LFP response recorded in the PAG and cerebellum.

Statistical analysis. Statistical analysis and graphs were performed with GraphPad Prism 9. Data are shown as mean ± S.E.M., except for rearing behaviour, USVs, duration of freezing and duration of movement which are plotted as median ± interquartile range (IQR). Paired t-tests or Wilcoxon test were used for within group comparisons, while unpaired t-tests or Mann Whitney test and ANOVA were used to compare groups. Differences were considered significant at $p < 0.05$. Pearson r correlation was used to compare the absolute change in freezing per animal from EE to LE vs the absolute change in unit area response from EE to LE. To investigate the relationship within animals between unit response size and freezing activity and the relationship between MCN and vPAG ERPs, repeated-measures correlation (using RStudio, see Bakdash et al., 2017) was calculated between response Area at tone onset and offset and percentage of time spent freezing during blocks of 7 tones (i.e. block 1 = tone 1-7; block 2 = tone 8-14 etc).

Methodological considerations

Our experiments were confined to the study of adult male rats. Gender differences are an important issue and an increasing body of evidence suggests there are neurobiological differences between male and female rodents in fear processing (Hurley et al., 2008; Bangasser et al., 2021). The extent to which such differences influenced our findings remains an open question for future study.

With regard to interventionist approaches our experiments included muscimol to block MCN activity during consolidation and this induced ataxia. It is possible that the stress and anxiety of the ataxia may have interfered with the newly formed fear memory leading to the electrophysiological and behavioural effects we observed in extinction training. However, we consider muscimol induced fear/stress is unlikely to fully explain our findings for the following reasons:

UOB Confidential

(i) The ataxia induced by the muscimol infusion into MCN during consolidation ranged across animals from mild to moderate. There was no difference between these animals and the amount of conditioned freezing displayed during retrieval, suggesting that fear learning was not related to the severity of the ataxia. More generally, we detected no change in the proportion of total time spent freezing during retrieval, suggesting that the ataxia during consolidation had little or no effect on fear learning.

(ii) The effect of muscimol infusion into MCN was specific to PAG encoding of CS+ tone offset and not CS+ tone onset. If our findings were due to a generalized disruption of fear learning because of fear/stress during consolidation, then it might be expected that this would affect both onset and offset response.

(iii) In relation to anxiety, Oksztel et al. (2002) found that systemic administration of muscimol in rats causes a general decrease in motility but has no effect on anxiety levels. And in terms of stress, previous studies (Brinks et al., 2009; Uwaya et al., 2016; Pietersen et al., 2016; Lesuis et al., 2018) have reported a correlation between the amount of freezing and corticosterone levels. Given that the amount of conditioned freezing behaviour was unaffected in our experiments, this suggests that stress is also unlikely to fully explain our findings.

An additional methodological consideration is that we used muscimol to abolish all outflow from MCN (which will include both direct and indirect pathways to the PAG), while we used the DREADD method to specifically inhibit modulate the direct pathway from MCN to ventrolateral PAG. Our experimental design therefore allowed a comparison between blocking all MCN pathways and a specific pathway targeting ventrolateral PAG. The muscimol was delivered during consolidation, while in the DREADD experiments CNO was delivered just prior to acquisition so was likely to include both a period during and after acquisition (i.e. to also include early consolidation, Jendryka et al., 2019). This means there was likely to be some overlap in the time course of action of the two types of manipulation (i.e. effects on early consolidation for both DREADD and muscimol). The DREADD method has recently been used in mice at different time points during fear conditioning, including the consolidation period after acquisition (Frontera et al., 2020). Like our muscimol results no effects on the proportion of total time spent freezing during extinction were reported, suggesting that the two methods are comparable. This also suggests that the behavioural effects we found in our DREADD experiments are likely to be related more to an action on associative memory processes during acquisition rather than during consolidation.

Finally, in terms of our finding that the emission of USVs was highly variable between animals, several studies have reported that only about half of animals emit 22 kHz USVs during fear conditioning (Wöhr

UOB Confidential

et al., 2005, 2008; Borta et al., 2006; Schwarting et al., 2012). The factors that underlie this variability are unknown, although they may include anxiety state, social experience and status (Hegoburu et al., 2011; Schwarting et al., 2012).

Acknowledgments: We gratefully acknowledge Ms Rachel Bissett for her expert help with histological processing and the Wolfson Bioimaging Facility for their support and assistance. We would like to thank Bryan Roth and Edward Boyden for supplying the viral vectors used in this work. This work was supported by BBSRC grant BB/MO19616/1 and a Wellcome Trust PhD studentship 203775/Z/16/Z.

Competing interests: The authors declare that no competing interests exist.

References:

An, Bandler, Öngür, & Price. (1998). Prefrontal cortical projections to longitudinal columns in the midbrain periaqueductal gray in macaque monkeys. *Journal of Comparative Neurology*, *401*(4), 455–479. https://doi.org/10.1002/(SICI)1096-9861(19981130)401:4<455::AID-CNE3>3.0.CO;2-6

Apps, & Strata. (2015). Neuronal circuits for fear and anxiety — the missing link. *Nature Reviews Neuroscience*, *16*(SEPTEMBER), 4–6. https://doi.org/10.1038/nrn4028

Asdourian, & Frerichs. (1970). Some effects of cerebellar stimulation. *Psychonomic Science*, *18*(5), 261–262. https://doi.org/10.3758/BF03331817

Bakdash, & Marusich. (2017). Repeated Measures Correlation. *Frontiers in Psychology*, *8*(MAR). https://doi.org/10.3389/FPSYG.2017.00456

Bangasser, & Cuarenta. (2021). Sex differences in anxiety and depression: circuits and mechanisms. *Nature Reviews. Neuroscience*. https://doi.org/10.1038/S41583-021-00513-0

Bares, Lungu, Liu, Waechter, Gomez, & Ashe. (2007). Impaired predictive motor timing in patients with cerebellar disorders. *Experimental Brain Research*, *180*(2), 355–365. https://doi.org/10.1007/s00221-007-0857-8

Blanchard, & Blanchard. (1969). Crouching as an index of fear. *Journal of Comparative and Physiological Psychology*, *67*(3), 370–375. https://doi.org/10.1037/h0026779

Born, Hitzler, Pietrowsky, Pauschinger, & Fehm. (1989). Influences of cortisol on auditory evoked potentials (AEPs) and mood in humans. *Neuropsychobiology*, *20*(3), 145–151. https://doi.org/10.1159/000118489

Borta, Wöhr, & Schwarting. (2006). Rat ultrasonic vocalization in aversively motivated situations and the role of individual differences in anxiety-related behavior. *Behavioural Brain Research*, *166*(2), 271–280. https://doi.org/10.1016/J.BBR.2005.08.009

Bremner, Staib, Kaloupek, Southwick, Soufer, & Charney. (1999). Neural correlates of exposure to traumatic pictures and sound in Vietnam combat veterans with and without posttraumatic stress disorder: A positron emission tomography study. *Biological Psychiatry*, *45*(7), 806–816. https://doi.org/10.1016/S0006-3223(98)00297-2

UOB Confidential

Brinks, de Kloet, & Oitzl. (2009). Corticosterone facilitates extinction of fear memory in BALB/c mice but strengthens cue related fear in C57BL/6 mice. *Experimental Neurology*, *216*(2), 375–382. https://doi.org/10.1016/J.EXPNEUROL.2008.12.011

Cacciola, Bertino, Basile, Di Mauro, Calamuneri, Chillemi, Duca, Bruschetta, Flace, Favaloro, Calabrò, Anastasi, & Milardi. (2019). Mapping the structural connectivity between the periaqueductal gray and the cerebellum in humans. *Brain Structure and Function*, *224*(6), 2153–2165. https://doi.org/10.1007/s00429-019-01893-x

Carrive, Leung, Harris, & Paxinos. (1997). Conditioned fear to context is associated with increased Fos expression in the caudal ventrolateral region of the midbrain periaqueductal gray. *Neuroscience*, *78*(1), 165–177. https://doi.org/10.1016/S0306-4522(97)83047-3

Cheron, Márquez-Ruiz, & Dan. (2016). Oscillations, Timing, Plasticity, and Learning in the Cerebellum. In *Cerebellum* (Vol. 15, Issue 2, pp. 122–138). Springer New York LLC. https://doi.org/10.1007/s12311-015-0665-9

Clelland, Choi, Romberg, Jr, Fragniere, & Tyers. (2010). *NIH Public Access*. *325*(5937), 210–213. https://doi.org/10.1126/science.1173215.A

D'Angelo. (2018). Physiology of the cerebellum. In *Handbook of Clinical Neurology* (Vol. 154, pp. 85–108). Elsevier B.V. https://doi.org/10.1016/B978-0-444-63956-1.00006-0

Frontera, Aissa, Sala, Mailhes-Hamon, Georgescu, Léna, & Popa. (2020). Bidirectional control of fear memories by cerebellar neurons projecting to the ventrolateral periaqueductal grey. *Nature Communications 2020 11:1*, *11*(1), 1–17. https://doi.org/10.1038/s41467-020-18953-0

Fujita-Jimbo, & Momoi. (2014). Specific expression of FOXP2 in cerebellum improves ultrasonic vocalization in heterozygous but not in homozygous Foxp2 (R552H) knock-in pups. *Neuroscience Letters*, *566*, 162–166. https://doi.org/10.1016/j.neulet.2014.02.062

Fujita, Tanabe, Imhof, Momoi, & Momoi. (2012). Cadm1-Expressing synapses on Purkinje cell dendrites are involved in mouse ultrasonic vocalization activity. *PLoS ONE*, *7*(1). https://doi.org/10.1371/journal.pone.0030151

Fujita, Tanabe, Shiota, Ueda, Suwa, Momoi, & Momoi. (2008). Ultrasonic vocalization impairment of Foxp2 (R552H) knockin mice related to speech-language disorder and abnormality of Purkinje cells. *Proceedings of the National Academy of Sciences of the United States of America*, *105*(8), 3117–3122. https://doi.org/10.1073/pnas.0712298105

Gilmartin, Balderston, & Helmstetter. (2014). Prefrontal cortical regulation of fear learning. *Trends in Neurosciences*, *37*(8), 455–464. https://doi.org/10.1016/j.tins.2014.05.004

Harris, Golder, & Likhtik. (2017). Multisite Electrophysiology Recordings in Mice to Study Cross-Regional Communication During Anxiety. In *Current Protocols in Neuroscience* (pp. 8.40.1-8.40.21). John Wiley & Sons, Inc. https://doi.org/10.1002/cpns.32

Haufler, Nagy, & Pare. (2013). Neuronal correlates of fear conditioning in the bed nucleus of the stria terminalis. *Learning and Memory*, *20*(11), 633–641. https://doi.org/10.1101/lm.031799.113

Hegoburu, Shionoya, Garcia, Messaoudi, Thévenet, & Mouly. (2011). The RUB cage: Respiration-ultrasonic vocalizations-behavior acquisition setup for assessing emotional memory in rats. *Frontiers in Behavioral Neuroscience*, *MAY*. https://doi.org/10.3389/FNBEH.2011.00025

Heinricher, Cheng, & Fields. (1987). Evidence for two classes of nociceptive modulating neurons in the periaqueductal gray. *Journal of Neuroscience*, *7*(1), 271–278. https://doi.org/10.1523/jneurosci.07-01-00271.1987

UOB Confidential

Herry, Ferraguti, Singewald, Letzkus, Ehrlich, & Lüthi. (2010). Neuronal circuits of fear extinction. In *European Journal of Neuroscience* (Vol. 31, Issue 4, pp. 599–612). Eur J Neurosci. https://doi.org/10.1111/j.1460-9568.2010.07101.x

Hirschberg, Li, Randall, Kremer, & Pickering. (2017). Functional dichotomy in spinal- vs prefrontal-projecting locus coeruleus modules splits descending noradrenergic analgesia from ascending aversion and anxiety in rats. *ELife*, *6*, e29808. https://doi.org/10.7554/eLife.29808

Holstege, Meiners, & Tan. (1985). Projections of the bed nucleus of the stria terminalis to the mesencephalon, pons, and medulla oblongata in the cat. *Experimental Brain Research*, *58*(2), 379–391. https://doi.org/10.1007/BF00235319

Hurley, & Adams. (2008). Sex, Gender, and Pain: An Overview of a Complex Field. *Anesthesia and Analgesia*, *107*(1), 309. https://doi.org/10.1213/01.ANE.0B013E31816BA437

Ivry. (1997). *Cerebellar timing systems*. https://doi.org/10.1016/S0074-7742(08)60370-0

Jendryka, Palchaudhuri, Ursu, van der Veen, Liss, Kätzel, Nissen, & Pekcec. (2019). Pharmacokinetic and pharmacodynamic actions of clozapine-N-oxide, clozapine, and compound 21 in DREADD-based chemogenetics in mice. *Scientific Reports*, *9*(1). https://doi.org/10.1038/s41598-019-41088-2

Ji, Yakhnitsa, Kiritoshi, Presto, & Neugebauer. (2018). Fear extinction learning ability predicts neuropathic pain behaviors and amygdala activity in male rats. *Molecular Pain*, *14*. https://doi.org/10.1177/1744806918804441

Johansen, Tarpley, LeDoux, & Blair. (2010). Neural substrates for expectation-modulated fear learning in the amygdala and periaqueductal gray. *Nature Neuroscience*, *13*(8), 979–986. https://doi.org/10.1038/nn.2594

Johansson, Hesslow, & Medina. (2016). Mechanisms for motor timing in the cerebellar cortex. In *Current Opinion in Behavioral Sciences* (Vol. 8, pp. 53–59). Elsevier Ltd. https://doi.org/10.1016/j.cobeha.2016.01.013

Kim, Horovitz, Pellman, Tan, Li, Richter-Levin, & Kim. (2013). Dorsal periaqueductal gray-amygdala pathway conveys both innate and learned fear responses in rats. *Proceedings of the National Academy of Sciences of the United States of America*, *110*(36), 14795–14800. https://doi.org/10.1073/pnas.1310845110

Koch, Oliveri, Torriero, Salerno, Gerfo, & Caltagirone. (2007). Repetitive TMS of cerebellum interferes with millisecond time processing. *Experimental Brain Research*, *179*(2), 291–299. https://doi.org/10.1007/s00221-006-0791-1

Koutsikou, Crook, Earl, Leith, Watson, Lumb, & Apps. (2014). Neural substrates underlying fear-evoked freezing: the periaqueductal grey-cerebellar link. *The Journal of Physiology*, *592*(10), 2197–2213. https://doi.org/10.1113/jphysiol.2013.268714

Lesuis, Catsburg, Lucassen, & Krugers. (2018). Effects of corticosterone on mild auditory fear conditioning and extinction; role of sex and training paradigm. *Learning & Memory (Cold Spring Harbor, N.Y.)*, *25*(10), 544–549. https://doi.org/10.1101/LM.047811.118

Liu, Whiteway, Sheikhattar, Butts, Babadi, & Kanold Correspondence. (2019). Parallel Processing of Sound Dynamics across Mouse Auditory Cortex via Spatially Patterned Thalamic Inputs and Distinct Areal Intracortical Circuits. *CellReports*, *27*, 872-885.e7. https://doi.org/10.1016/j.celrep.2019.03.069

Luong, Carlisle, Southwell, & Patterson. (2011). Assessment of motor balance and coordination in

UOB Confidential

mice using the balance beam. *Journal of Visualized Experiments : JoVE*, *49*. https://doi.org/10.3791/2376

McNally, Johansen, & Blair. (2011). Placing prediction into the fear circuit. *Trends in Neurosciences*, *34*(6), 283–292. https://doi.org/10.1016/j.tins.2011.03.005

Milad, & Quirk. (2012). Fear extinction as a model for translational neuroscience: Ten years of progress. In *Annual Review of Psychology* (Vol. 63, pp. 129–151). NIH Public Access. https://doi.org/10.1146/annurev.psych.121208.131631

Nisimaru, Mittal, Shirai, Sooksawate, Anandaraj, Hashikawa, Nagao, Arata, Sakurai, Yamamoto, & Ito. (2013). Orexin-neuromodulated cerebellar circuit controls redistribution of arterial blood flows for defense behavior in rabbits. *Proceedings of the National Academy of Sciences of the United States of America*, *110*(35), 14124–14131. https://doi.org/10.1073/pnas.1312804110

Oksztel, Car, & Wioeniewski. (2002). *MUSCIMOL CHANGES HYPOXIA-INDUCED IMPAIRMENT OF BEHAVIOR IN RATS*.

Ouda, Jílek, & Syka. (2016). Expression of c-Fos in rat auditory and limbic systems following 22-kHz calls. *Behavioural Brain Research*, *308*, 196–204. https://doi.org/10.1016/j.bbr.2016.04.030

Ozawa, Ycu, Kumar, Yeh, Ahmed, Koivumaa, & Johansen. (2017). A feedback neural circuit for calibrating aversive memory strength. *Nature Neuroscience*, *20*(1), 90–97. https://doi.org/10.1038/nn.4439

Pellow, Chopin, File, & Briley. (1985). Validation of open : closed arm entries in an elevated plus-maze as a measure of anxiety in the rat. *Journal of Neuroscience Methods*, *14*(3), 149–167. https://doi.org/10.1016/0165-0270(85)90031-7

Pietersen, Bosker, Postema, & Boer. (2016). Fear conditioning and shock intensity: the choice between minimizing the stress induced and reducing the number of animals used: *Http://Dx.Doi.Org/10.1258/002367706776319006*, *40*(2), 180–185. https://doi.org/10.1258/002367706776319006

Qin, Chimoto, Sakai, Wang, & Sato. (2007). Comparison Between Offset and Onset Responses of Primary Auditory Cortex – Neurons in Awake Cats. *Journal of Neurophysiology*, *97*(5), 3421–3431. https://doi.org/10.1152/jn.00184.2007

Quirk, Armony, & LeDoux. (1997). Fear conditioning enhances different temporal components of tone-evoked spike trains in auditory cortex and lateral amygdala. *Neuron*, *19*(3), 613–624. https://doi.org/10.1016/S0896-6273(00)80375-X

Rescorla, R. Wagner. (1972). A theory of Pavlovian conditioning: Variations in the effectiveness of reinforcement and nonreinforcement. *Classical Conditioning II: Current Research and Theory*, *January 1972*, 64–99.

Roy, Shohamy, Daw, Jepma, Wimmer, & Wager. (2014). Representation of aversive prediction errors in the human periaqueductal gray. *Nature Neuroscience*, *17*(11), 1607–1612. https://doi.org/10.1038/nn.3832

Sacchetti, B., Scelfo, & Strata. (2009). Cerebellum and emotional behavior. *Neuroscience*, *162*(3), 756–762. https://doi.org/10.1016/j.neuroscience.2009.01.064

Sacchetti, Benedetto, Baldi, Lorenzini, & Bucherelli. (2002). Cerebellar role in fear-conditioning consolidation. *Proceedings of the National Academy of Sciences of the United States of America*, *99*(12), 8406–8411. https://doi.org/10.1073/pnas.112660399

Sacchetti, Benedetto, Sacco, & Strata. (2007). Reversible inactivation of amygdala and cerebellum

UOB Confidential

but not perirhinal cortex impairs reactivated fear memories. *European Journal of Neuroscience*, *25*(9), 2875–2884. https://doi.org/10.1111/j.1460-9568.2007.05508.x

Sacchetti, Benedetto, Scelfo, & Strata. (2005). The cerebellum: Synaptic changes and fear conditioning. *Neuroscientist*, *11*(3), 217–227. https://doi.org/10.1177/1073858405276428

Sanders, Klein, Mayer, Heym, & Handwerker. (1980). Differential effects of noxious and non-noxious input on neurones according to location in ventral periaqueductal grey or dorsal raphe nucleus. *Brain Research*, *186*(1), 83–97. https://doi.org/10.1016/0006-8993(80)90257-7

Sandner, Schmitt, & Karli. (1987). Mapping of jumping, rearing, squealing and switch-off behaviors elicited by periaqueductal gray stimulation in the rat. *Physiology & Behavior*, *39*(3), 333–339. https://doi.org/10.1016/0031-9384(87)90231-9

Schmitzer-Torbert, Jackson, Henze, Harris, & Redish. (2005). Quantitative measures of cluster quality for use in extracellular recordings. *Neuroscience*, *131*(1), 1–11. https://doi.org/10.1016/j.neuroscience.2004.09.066

Scholl, Gao, & Wehr. (2010). Nonoverlapping Sets of Synapses Drive On Responses and Off Responses in Auditory Cortex. *Neuron*, *65*(3), 412–421. https://doi.org/10.1016/j.neuron.2010.01.020

Schwarting, & Wöhr. (2012). On the relationships between ultrasonic calling and anxiety-related behavior in rats. In *Brazilian Journal of Medical and Biological Research* (Vol. 45, Issue 4, pp. 337–348). Associação Brasileira de Divulgação Científica. https://doi.org/10.1590/S0100-879X2012007500038

Sharma, Sinha, Mathur, & Nayar. (1999). Neuronal responses of periaqueductal gray to peripheral noxious stimulation. *Indian Journal of Physiology and Pharmacology*, *43*(4), 449–457. https://europepmc.org/article/med/10776460

Sołyga, & Barkat. (2019). Distinct processing of tone offset in two primary auditory cortices. *Scientific Reports*, *9*(1), 1–12. https://doi.org/10.1038/s41598-019-45952-z

Spencer, & Ivry. (2013). Cerebellum and timing. In *Handbook of the Cerebellum and Cerebellar Disorders* (pp. 1201–1220). Springer Netherlands. https://doi.org/10.1007/978-94-007-1333-8_52

Stachniak, Ghosh, & Sternson. (2014). Chemogenetic Synaptic Silencing of Neural Circuits Localizes a Hypothalamus→Midbrain Pathway for Feeding Behavior. *Neuron*, *82*(4), 797–808. https://doi.org/10.1016/J.NEURON.2014.04.008

Strick, Dum, & Fiez. (2009). Cerebellum and Nonmotor Function. *Annual Review of Neuroscience*, *32*(1), 413–434. https://doi.org/10.1146/annurev.neuro.31.060407.125606

Supple, & Leaton. (1990). Cerebellar vermis: essential for classically conditioned bradycardia in the rat. *Brain Research*, *509*(1), 17–23. https://doi.org/10.1016/0006-8993(90)90303-S

Supple, Leaton, & Fanselow. (1987). Effects of cerebellar vermal lesions on species-specific fear responses, neophobia, and taste-aversion learning in rats. *Physiology & Behavior*, *39*(5), 579–586. https://doi.org/10.1016/0031-9384(87)90156-9

Takahashi, Nakao, & Kaga. (2004). Cortical mapping of auditory-evoked offset responses in rats. *NeuroReport*, *15*(10), 1565–1569. https://doi.org/10.1097/01.wnr.0000134848.63755.5c

Teune, van der Burg, van der Moer, Voogd, & Ruigrok. (2000). Topography of cerebellar nuclear projections to the brain stem in the rat. *Progress in Brain Research*, *124*, 141–172. https://doi.org/10.1016/S0079-6123(00)24014-4

UOB Confidential

Tian, Kuśmierek, & Rauschecker. (2013). Analogues of simple and complex cells in rhesus monkey auditory cortex. *Proceedings of the National Academy of Sciences of the United States of America*, *110*(19), 7892–7897. https://doi.org/10.1073/pnas.1221062110

Toledo, Lang, Doengi, Morrison, Stein, & Baader. (2019). Merlin modulates process outgrowth and synaptogenesis in the cerebellum. *Brain Structure and Function*, *224*(6), 2121–2142. https://doi.org/10.1007/s00429-019-01897-7

Tovote, Esposito, Botta, Chaudun, Fadok, Markovic, Wolff, Ramakrishnan, Fenno, Deisseroth, Herry, Arber, & Lüthi. (2016). Midbrain circuits for defensive behaviour. *Nature*, *534*(7606), 206–212. https://doi.org/10.1038/nature17996

Tovote, Fadok, & Lüthi. (2015). Neuronal circuits for fear and anxiety. *Nature Reviews Neuroscience*, *16*(6), 317–331. https://doi.org/10.1038/nrn3945

Umeda, Takashima, Nakagawa, Maekawa, Ikegami, Yoshikawa, Kobayashi, Okanoya, Inokuchi, & Osumi. (2010). Evaluation of pax6 mutant rat as a model for autism. *PLoS ONE*, *5*(12). https://doi.org/10.1371/journal.pone.0015500

Utz, Thürling, Ernst, Hermann, Stark, Wolf, Timmann, & Merz. (2015). Cerebellar vermis contributes to the extinction of conditioned fear. *Neuroscience Letters*, *604*, 173–177. https://doi.org/10.1016/J.NEULET.2015.07.026

Uwaya, Lee, Park, Lee, Muto, Nakajima, Ohta, & Mikami. (2016). Acute immobilization stress following contextual fear conditioning reduces fear memory: timing is essential. *Behavioral and Brain Functions 2016 12:1*, *12*(1), 1–13. https://doi.org/10.1186/S12993-016-0092-1

Vaaga, Brown, & Raman. (2020). Cerebellar modulation of synaptic input to freezing-related neurons in the periaqueductal gray. *ELife*, *9*. https://doi.org/10.7554/eLife.54302

Vianna, Graeff, Brandão, & Landeira-Fernandez. (2001). Defensive freezing evoked by electrical stimulation of the periaqueductal gray: comparison between dorsolateral and ventrolateral regions. *Neuroreport*, *12*(18), 4109–4112. http://www.ncbi.nlm.nih.gov/pubmed/11742247

Walker, D. L., Ressler, Lu, & Davis. (2002). Facilitation of conditioned fear extinction by systemic administration or intra-amygdala infusions of D-cycloserine as assessed with fear-potentiated startle in rats. *The Journal of Neuroscience : The Official Journal of the Society for Neuroscience*, *22*(6), 2343–2351. https://doi.org/10.1523/jneurosci.1828-04.2004

Walker, P., & Carrive. (2003). Role of ventrolateral periaqueductal gray neurons in the behavioral and cardiovascular responses to contextual conditioned fear and poststress recovery. *Neuroscience*, *116*(3), 897–912. https://doi.org/10.1016/S0306-4522(02)00744-3

Walker, R. A., Wright, Jhou, & McDannald. (2019). The ventrolateral periaqueductal grey updates fear via positive prediction error. *European Journal of Neuroscience*, *51*(3), 866–880. https://doi.org/10.1111/ejn.14536

Wang, Chen, Xu, Sun, Chen, Zhao, Luo, Liu, Guo, Xie, Zhong, Bai, Tian, Mao, Ye, Tao, Li, Farzinpour, Li, … Zhang. (2019). Direct auditory cortical input to the lateral periaqueductal gray controls sound-driven defensive behavior. *PLOS Biology*, *17*(8), e3000417. https://doi.org/10.1371/journal.pbio.3000417

Watson, Cerminara, Lumb, & Apps. (2016). Neural correlates of fear in the periaqueductal gray. *Journal of Neuroscience*, *36*(50), 12707–12719. https://doi.org/10.1523/JNEUROSCI.1100-16.2016

Wei, & Kording. (2018). Behavioral tracking gets real. *Nature Neuroscience*, 1.

UOB Confidential

https://doi.org/10.1038/s41593-018-0215-0

Whiteside, & Snider. (1953). Relation of cerebellum to upper brain stem. *Journal of Neurophysiology*, *16*(4), 397–413. https://doi.org/10.1152/jn.1953.16.4.397

Wöhr, Borta, & Schwarting. (2005). Overt behavior and ultrasonic vocalization in a fear conditioning paradigm: A dose–response study in the rat. *Neurobiology of Learning and Memory*, *84*(3), 228–240. https://doi.org/10.1016/J.NLM.2005.07.004

Wöhr, & Schwarting. (2008). Ultrasonic calling during fear conditioning in the rat: no evidence for an audience effect. *Animal Behaviour*, *76*(3), 749–760. https://doi.org/10.1016/J.ANBEHAV.2008.04.017

Wright, Jhou, Pimpinelli, & McDannald. (2019). Cue-inhibited ventrolateral periaqueductal gray neurons signal fear output and threat probability in male rats. *ELife*, *8*, 1–16. https://doi.org/10.7554/elife.50054

Wright, & McDannald. (2019). Ventrolateral periaqueductal gray neurons prioritize threat probability over fear output. *ELife*, *8*. https://doi.org/10.7554/eLife.45013

Xu, Liu, Ashe, & Bushara. (2006). Role of the olivo-cerebellar system in timing. *Journal of Neuroscience*, *26*(22), 5990–5995. https://doi.org/10.1523/JNEUROSCI.0038-06.2006

UOB Confidential

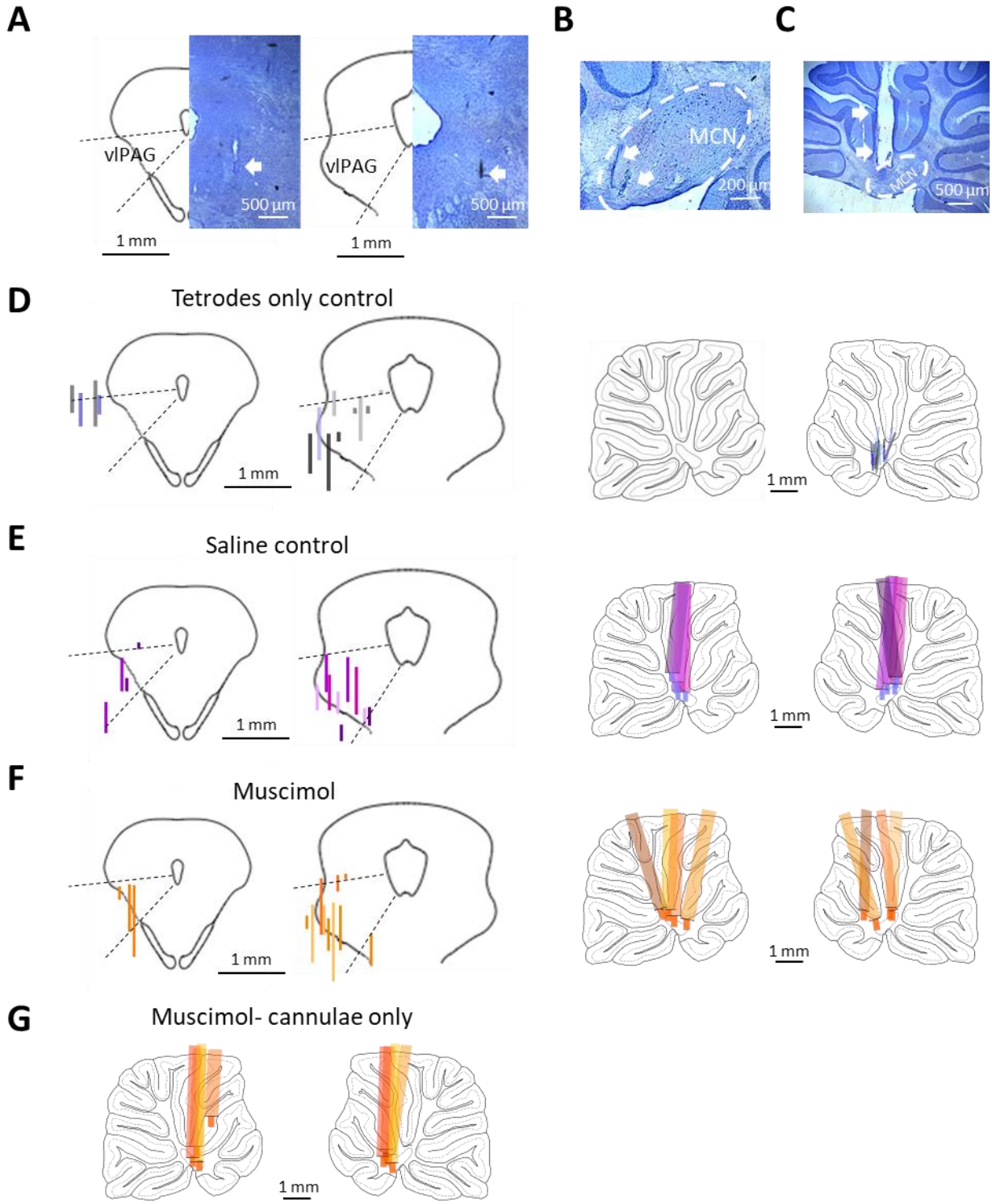

Supplementary Figure 1. Histological verification of implants. (A) Photomicrographs of two example tetrode tracks (arrows) in ventral PAG. Outlines show left half of two coronal sections (AP levels -6.5 and -7.5) of the periaqueductal grey. Dotted lines indicate approximate location of the ventrolateral sector (vlPAG). Note that a lack of correspondence between the physiological and histological boundaries of the lateral border of PAG has been reported previously (McMullan & Lumb 2006). (B) Same as A but tracks in sagittal sections (±1 mm of midline) medial cerebellar nucleus (MCN). and (C) example track of a cerebellar cannula. (D) Pairs of figurines to the left show two coronal sections (AP levels -6.5 and -7.5) of the periaqueductal grey. Pairs of figurines to the

UOB Confidential

right show sagittal sections of left and right cerebellum (±1 mm of midline). Tetrodes only controls (n = 6 rats, tetrodes implanted on one side of PAG and also in the contralateral MCN), tracks colour coded for each animal and length of each track indicates extent of unit recording in that track); reconstruction of tetrode tracks in the vPAG (left) and contralateral MCN (right). (E) Same as D but for saline controls (tetrodes implanted on one side in PAG and cannulae implanted bilaterally in MCN for saline infusion (n= 4 rats). In the cerebellar sections, the whole length of each cannula track has been reconstructed and the blue coloured tips indicate the extension of the internal cannula for infusions. (F) Same as E but cannulae used for infusion of muscimol (n= 4 rats). In the cerebellar tracks, orange coloured tips indicate the extension of the internal cannulae for infusions. (G) Same as F but only cannulae implanted in left and right cerebellum for infusion of muscimol (n=4 rats).

UOB Confidential

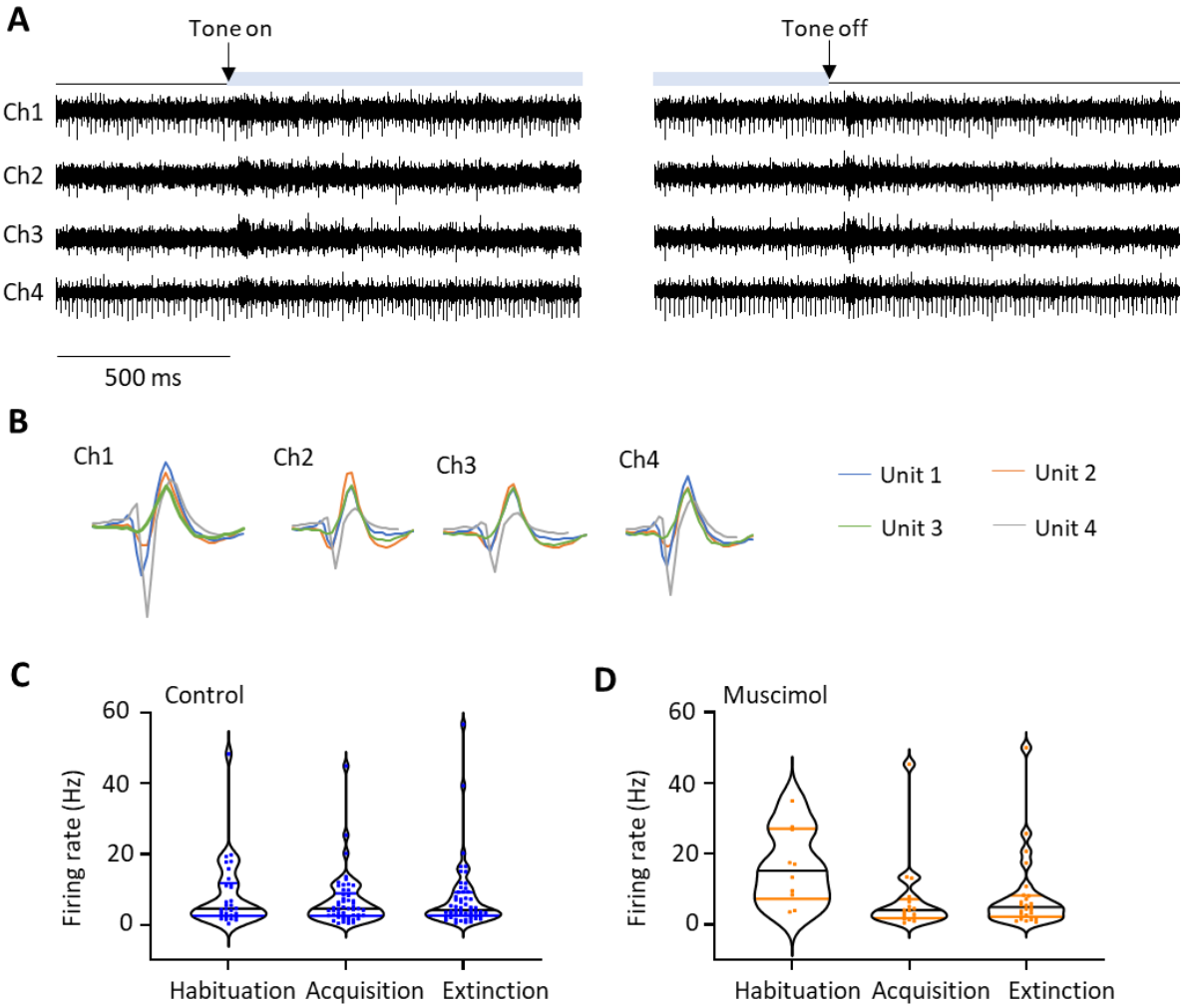

Supplementary Figure 2. **Tetrode recordings. (**A) Example electrophysiological data recorded from a vPAG tetrode (30kHz sampling rate, 600-3kHz bandpass filter, Ch1-4, tetrode channels 1-4). Raw data captured during early extinction training around the time of CS+ onset (left, tone on) and CS+ offset (right, tone off). Light blue bar shows time the tone is on. (B) Spikes were sorted using all channels in MClust to identify individual units; in this case 4 units (colour coded) were isolated. Individual units were classified as described in Methods. (C) Violin plots showing distribution of baseline firing rates for all available single units recorded in vPAG during three phases of fear conditioning: habituation (n=30 units); acquisition (n=50 control units); and extinction (n=55 control units). Horizontal black lines show median and blue lines IQR firing rate for each phase of conditioning. (D) Same as C, but for single units recorded during muscimol experiments. Habituation (n = 10 units); acquisition (n= 17 units); extinction (n= 25 units). Horizontal black lines show median and orange lines IQR firing rate for each phase of conditioning.

UOB Confidential

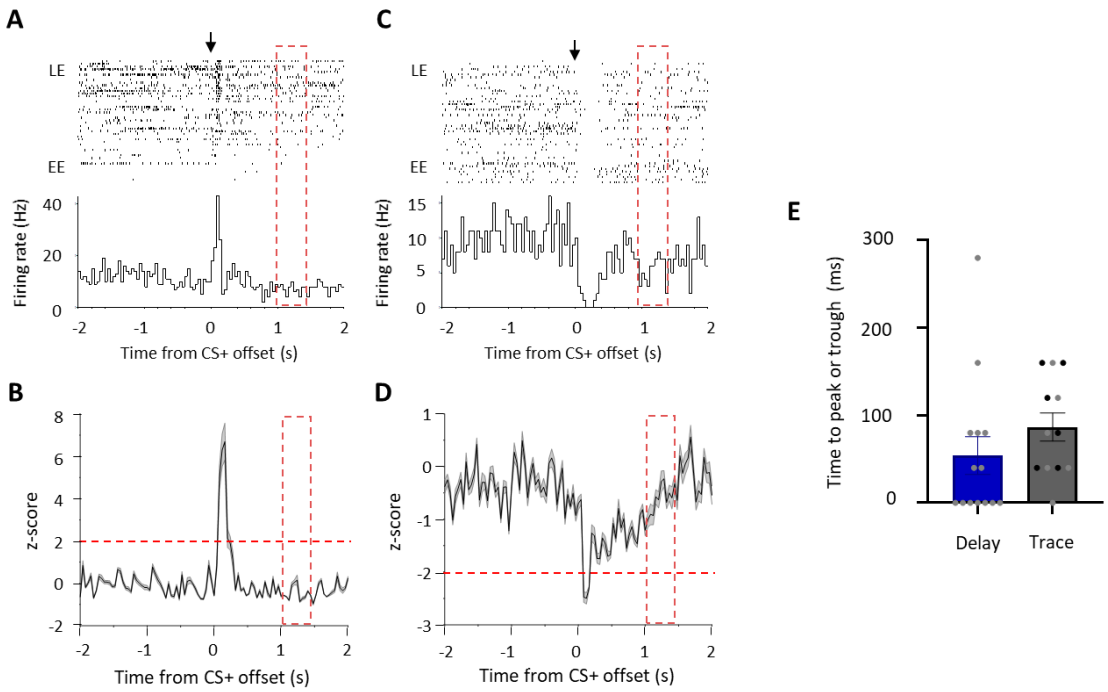

Supplementary Figure 3. vPAG offset responses during auditory cued fear trace conditioning. (A) Example type 1 offset unit in vPAG recorded during extinction following acquisition where a 1 second trace was introduced between CS offset and the US during acquisition. Raster plot and peri-event time histogram (PETH) showing activity relative to CS+ offset (arrow in raster and time zero in PETH). Time of the US during acquisition is shown by red dotted rectangle; 40ms bins. (B) Same as A but mean PETH ± SEM for all type 1 offset units (n = 6). Horizontal dashed red line represents significance level ($p<0.05$). (C) Same as A but example type 4 offset unit. (D) Same as B but mean PETH ± SEM for all type 4 offset units (n = 6). (E) Bar chart plotting mean time to peak or trough in activity for all units after CS+ offset (delay, n = 19 units recorded after delay conditioning; trace, n = 12 units recorded after trace conditioning; individual units for trace experiments: light grey type 1 offset units and dark grey type 4 offset units. No significant difference in timing between trace and delay ($p>0.05$).

UOB Confidential

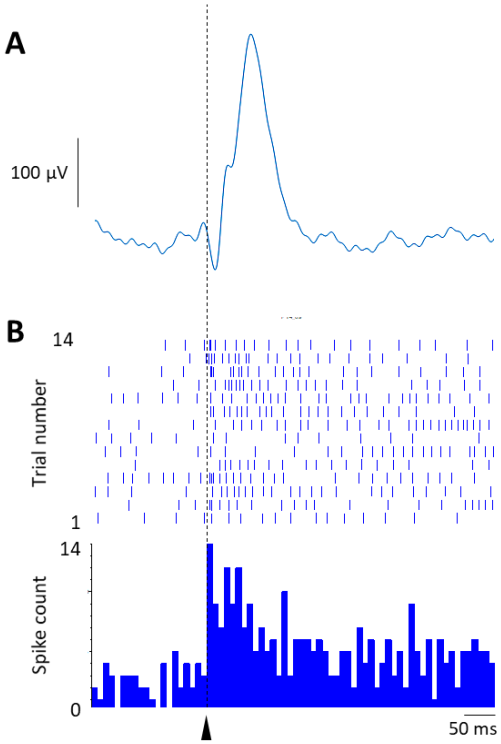

Supplementary Figure 4. Relationship between unit activity and event related potentials. (A) Example event related potential (ERP) recorded in the vPAG during early extinction training at CS+ offset. Average of 14 trials. (B) Example single unit data recorded simultaneously from the same vPAG recording site. Vertical dashed line and arrowhead indicate CS+ offset at time zero. Raster plot 14 trials, PETH, 10 ms bin width.

UOB Confidential

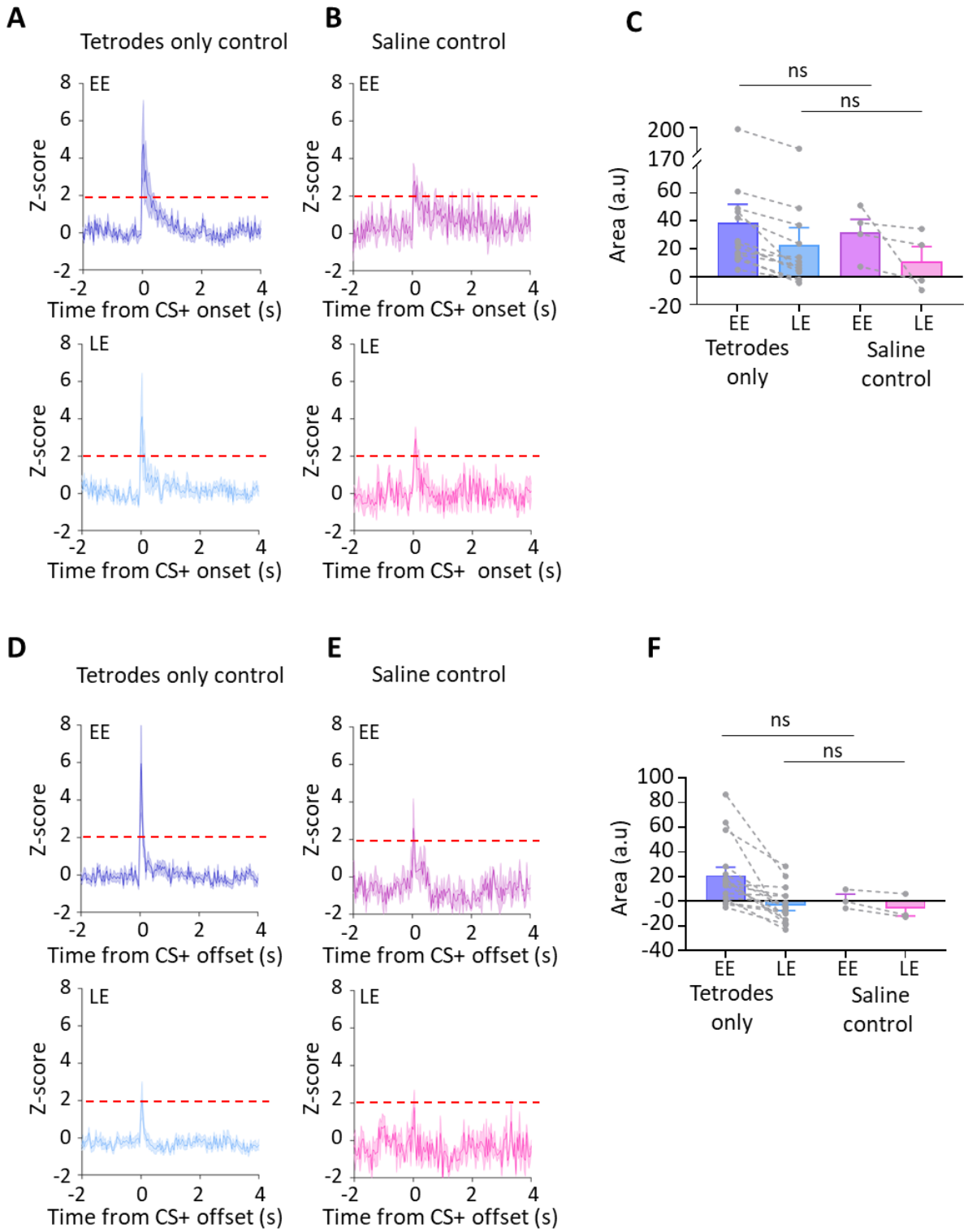

Supplementary Figure 5. Comparison of single unit results for tetrodes only versus saline control animals. (A) Group data for tetrodes only control animals (n = 14 units) recorded on day 2, showing average z-scored type 1 onset responses during early extinction (EE, upper panel) and late extinction (LE, lower panel). Time zero, CS+ tone onset. Solid lines in each plot show mean z-score, shaded regions ± SEM. Horizontal dashed red lines show significance level ($p<0.05$). (B) Same as A but grouped data for saline control animals recorded on day 3 (n = 4 units). (C) Bar charts showing average type 1 onset response area (arbitrary units) during EE and LE for single units recorded in tetrodes only and saline control animals. Pairs of data points connected with dashed lines show change in mean response area for each single unit over extinction training. Bars show group means

UOB Confidential

± SEM. ns, no significant difference (unpaired t test, EE, p = 0.785; LE, p = 0.635). D and E same as A and B but for type 1 offset responses. Time zero, CS+ tone offset. (D) Tetrodes only control unit offset responses recorded on day 2 (n = 16 units). (E) Saline control unit offset responses recorded on day 3 (n = 3 units). (F) Same as C. ns, no significant difference (unpaired t test, EE, p = 0.224 and LE, p = 0.824).

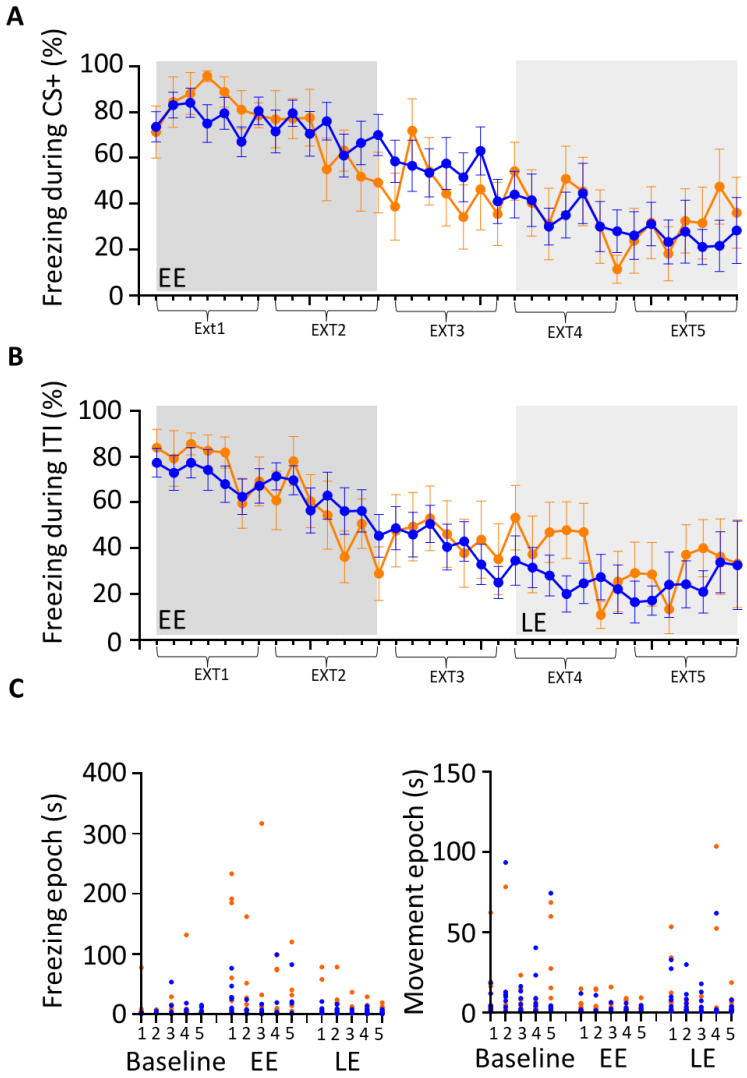

Supplementary Figure 6. Trial by trial comparison of conditioned behaviour in muscimol and control animals (A) Grouped data showing the average percentage of time spent freezing during presentation of each CS+ tone as a function of extinction training. Five blocks of extinction (Ext1-5) with early extinction (EE, ext1,2) shaded dark grey, and late extinction (LE, ext4,5), shaded light grey. Control data (blue, n= 10 rats) and muscimol data (orange, n=8 rats). Plots show mean ± SEM. (B) Same as A but during the inter-tone interval (ITI). (C) Scatterplots for baseline, EE and LE, showing the duration of the first 5 freezing epochs (left panel) and first 5 movement epochs (right panel) for each block of extinction training (1-5, see Methods for further details). Each data point represents the freezing or movement epoch for an individual animal. Control = blue, Muscimol = orange.

UOB Confidential

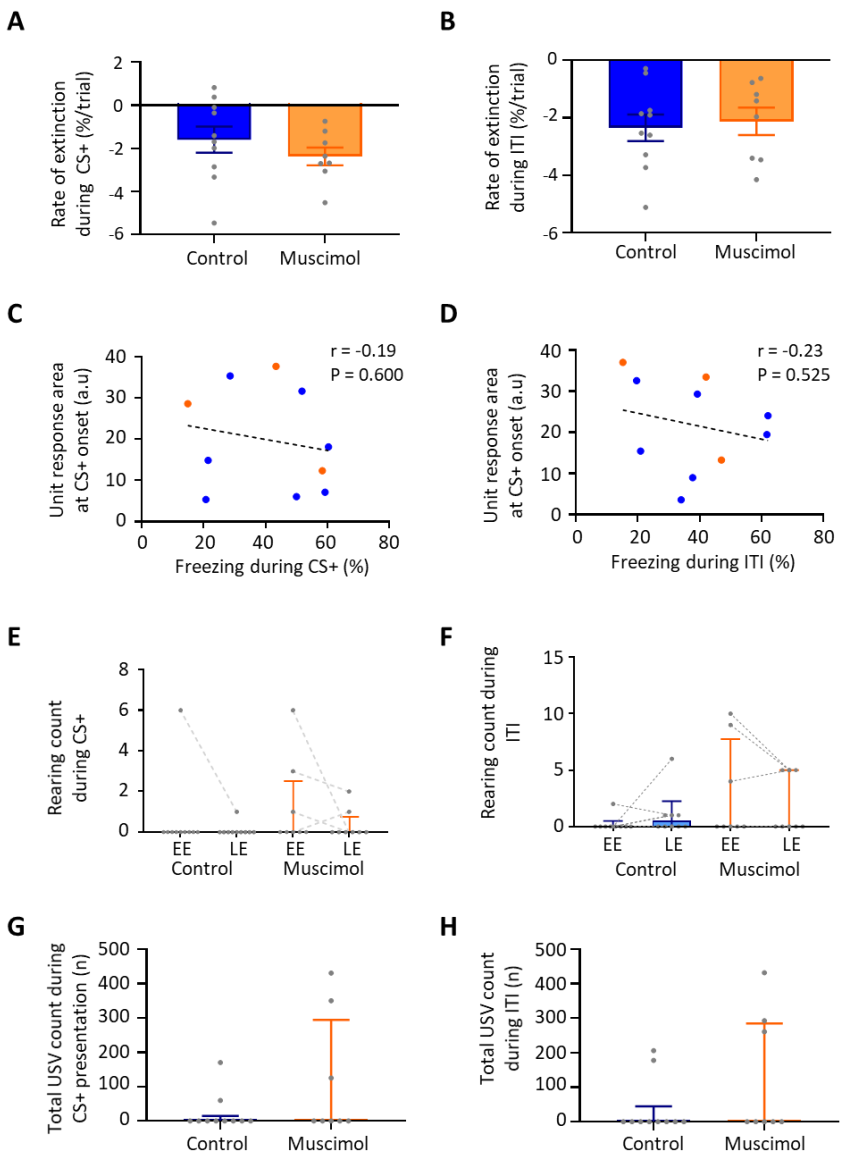

Supplementary Figure 7. Conditioned fear related behaviours. (A) Rate of extinction as measured by the slope of the line of best fit for change in percentage of time spent freezing during presentation of the CS+ over the first 21 presentations of the CS+ during extinction training in control (n = 10 rats) versus muscimol (n = 8 rats) experiments. Individual data points show mean rate of change per animal. Bars show group means ±SEM. (B) Same as A but the change in percentage of time spent freezing during the ITI for the first 21 CS+ presentations during extinction training in control (n =1 0 rats) versus muscimol (n = 8 rats) experiments. (C) Scatterplot showing the mean unit response area (arbitrary units) at CS+ onset as a function of percentage time spent freezing activity in EE and LE during CS+ presentation. Individual data points represent individual animals. Blue, control; orange, muscimol. Pearson correlation r = -0.19, p >0.05. (D) Same as C but for freezing during the ITI and unit response area at CS+ offset. Pearson correlation r = -0.23, p >0.05. (E) The total number of rears during CS+ presentation during extinction training in control (n = 10 rats) versus muscimol (n = 8 rats) experiments. Individual data points connected with dashed lines show change in mean number of rears per animal over extinction training. Bars show group median and IQR (EE, p = 0.275; LE, p = 0.444, Mann Whitney test). (F) Same as E but rearing count for ITI in control (n = 10 rats) versus muscimol (n = 8 rats) experiments (EE, p = 0.490. LE, p = 0.763, Mann Whitney test). (G) Total number of ultrasonic vocalisations (USVs) during presentation of the CS+ in all extinction training trials for control (n = 10 rats) versus muscimol (n = 8 rats) experiments. Individual data points show mean count per animal. Bars show group median and IQR (p = 0.321,

UOB Confidential

Mann Whitney test). (H) Same as G but USV count in the ITI for control (n = 10 rats) versus muscimol (n = 8 rats) experiments (p = 0.304, Mann-Whitney test).

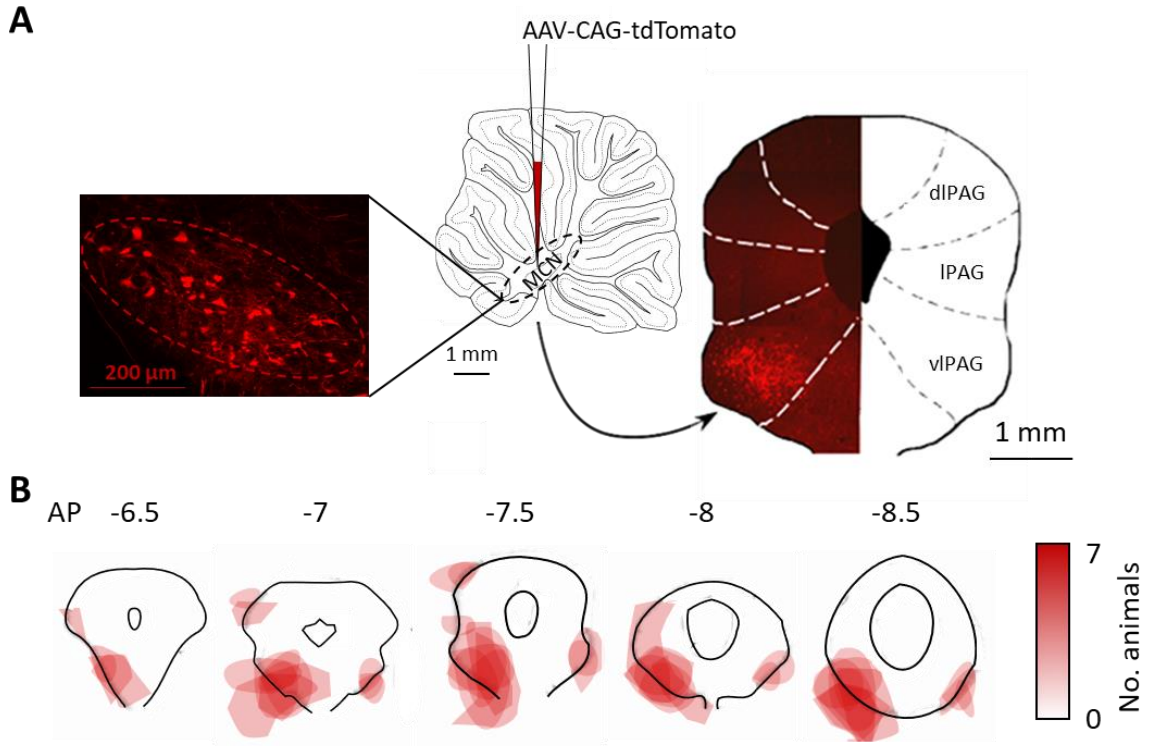

Supplementary Figure 8. Anatomical mapping of the MCN-PAG pathway. (A) Schematic showing on a sagittal section of the cerebellum injection into the MCN of an anterograde tracer (AAV-CAG-tdTomato viral vector). To the left high power photomicrograph showing transfected neurons in MCN. To the right, coronal section shows representative pattern of terminal labelling in the contralateral PAG in one animal (dlPAG, lPAG, vlPAG; dorsolateral, lateral and ventrolateral periaqueductal grey). (B) Coronal sections of the PAG at different anteroposterior (AP) levels showing the pattern of terminal labelling in all available animals (n = 7 rats). The darker the red shading the larger the number of animals with terminal labelling in that area.

UOB Confidential

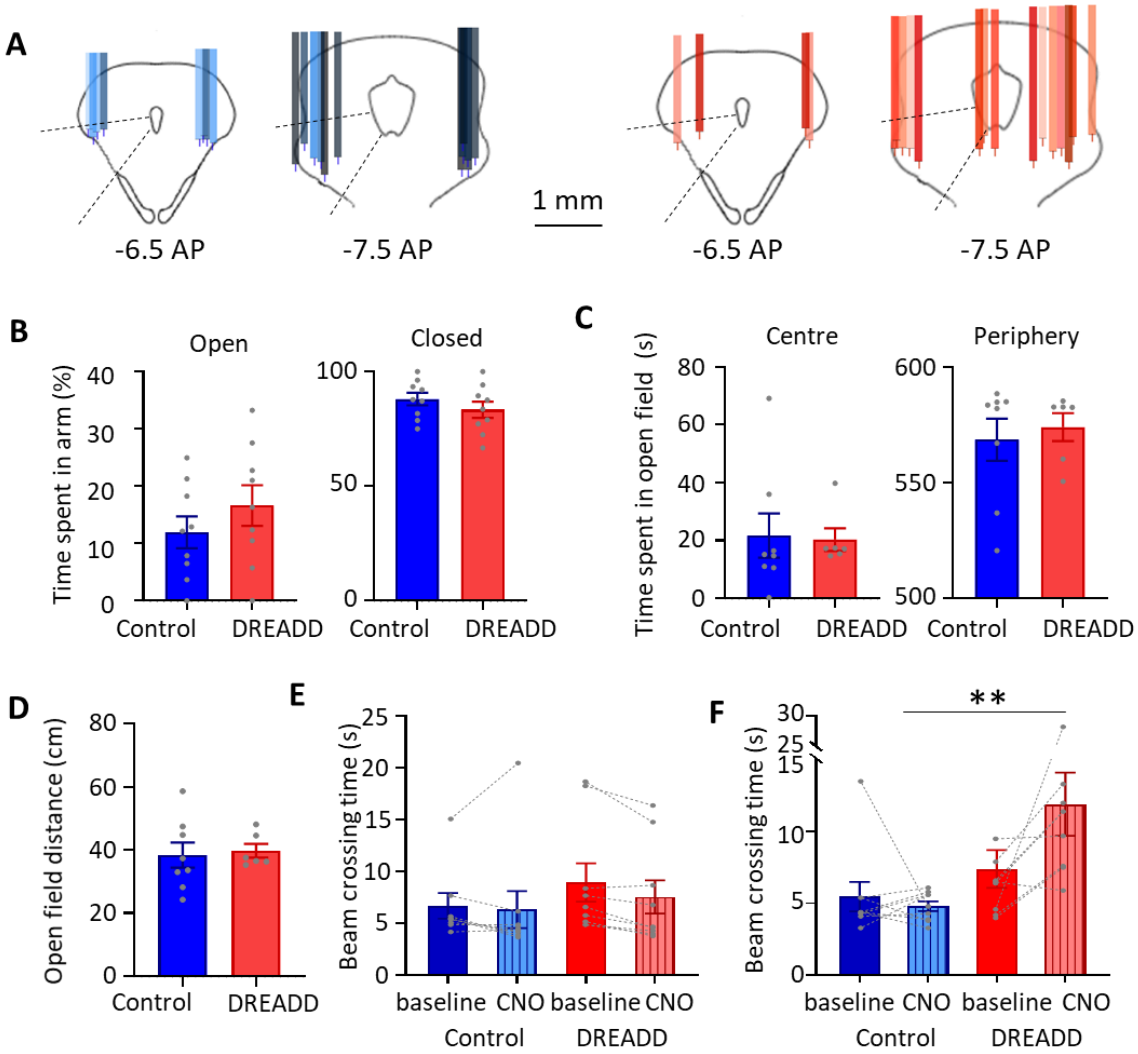

Supplementary Figure 9. Effect of DREADDs on general motor and affective behaviour. (A) Histological reconstruction of cannulae placement in PAG in control (n = 9 rats, tracks colour coded blue to black for different animals) and DREADD animals (n = 10 rats, tracks colour coded orange to red for different animals). For each track the tips indicate the extension of the internal cannula for infusions. (B) Percentage of the total time in an elevated plus maze spent in the open arm (left) and in the closed arm (right) for control (n=9 rats) versus DREADD (n = 9 rats) experiments. Individual data points show percentage of time per animal. Bars show mean ± SEM (open arm, p = 0.635; closed arm, p=0.316; unpaired t-test). (C) Time spent in the centre versus the periphery of the open field arena for control versus DREADD animals. Individual data points show total time per animal. Bars show mean ± SEM (centre p = 0.887; periphery p = 0.651, unpaired t-test). (D) The total distance moved in the open field arena in control (n = 8 rats) versus DREADD (n = 6 rats) experiments. Individual data points show total distance per animal. Bars show mean ± SEM (p = 0.794, unpaired t-test). (E) Beam walking traversal times in control (n = 9 rats) and DREADD (n = 9 rats) experiments before (baseline) and after infusion of CNO into vPAG for the two groups of animals. Pairs of data points connected by dotted lines show change in mean crossing time per animal between baseline and CNO. Bars show mean ± SEM (time to traverse, p = 0.618, unpaired t-test; number of foot slips, p = 0.500, Mann-Whitney test). (F) Same as E but beam traversal times in control (n = 9 rats) and DREADD (n = 9 rats) experiments before (baseline) and intraperitoneal injection of CNO. Unpaired t-test **, p < 0.001.

UOB Confidential

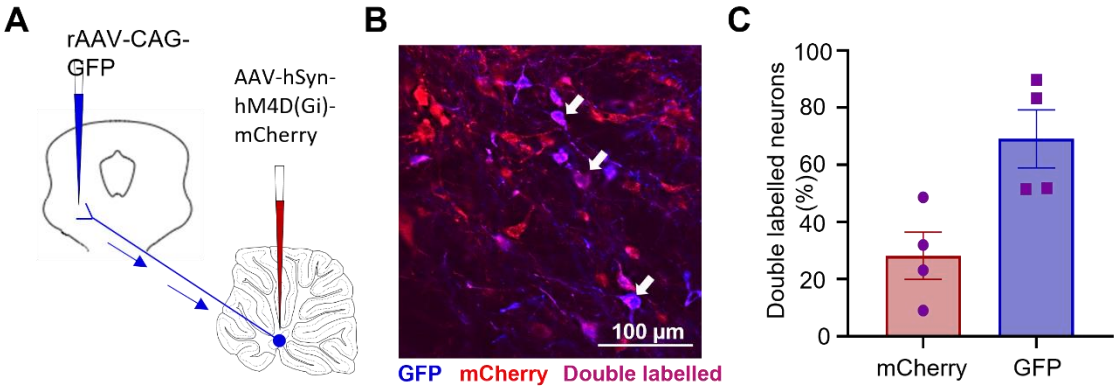

Supplementary Figure 10. Anatomical and physiological evaluation of DREADD transfection of MCN-PAG pathway. (A) Schematic showing experimental arrangement for anatomical assessment of DREADD transfection. In each animal a green fluorescent retrograde tracer (rAAV-CAG-GFP) was injected into the ventrolateral sector of PAG (shown as false colour blue) and in the same animals MCN was transfected with inhibitory DREADD virus that expressed red fluorescence (AAV-hSyn-hM4D(Gi)-mCherry). (B) Photomicrograph showing examples of single (red or blue) and double labelled neurons (purple, arrows) in MCN. (C) Graph plotting double labelled neurons in MCN as a percentage of the two single labelled populations (n= 4 rats). Individual data points per animal. Mean ± SEM.

UOB Confidential

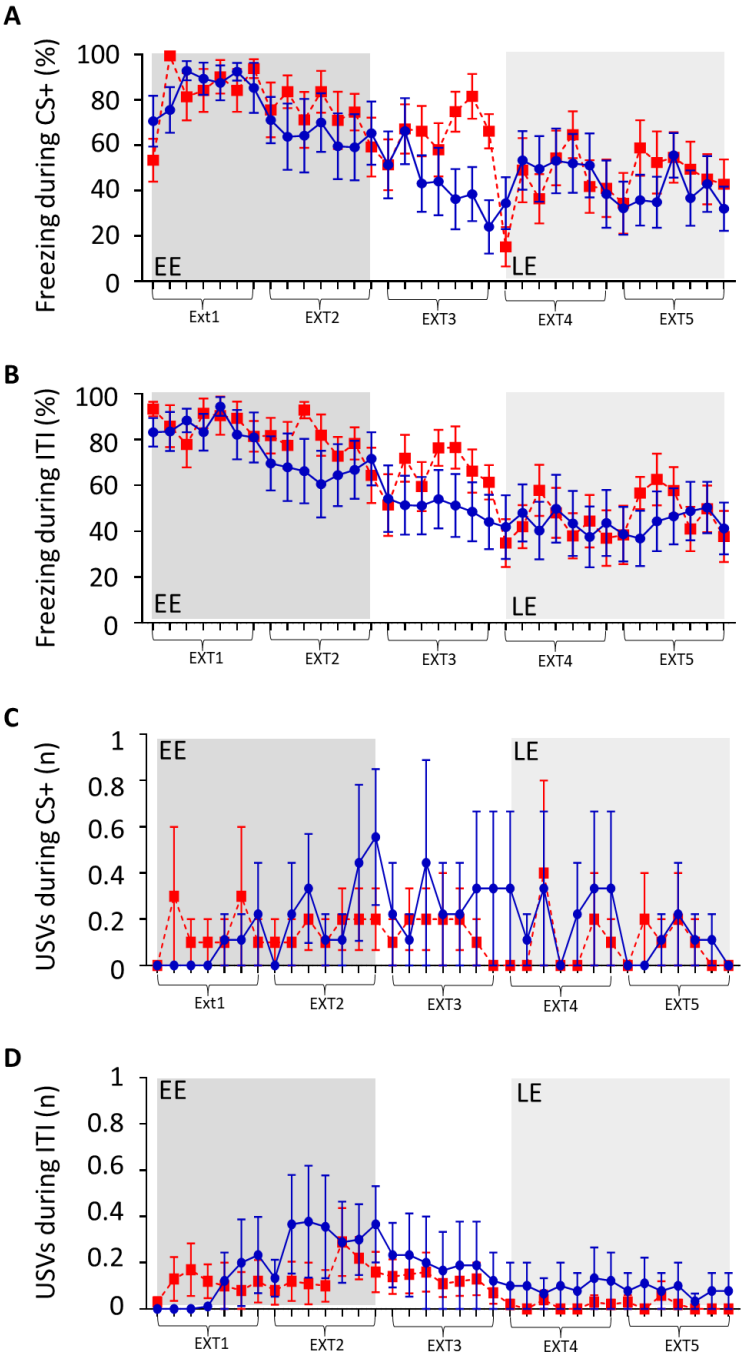

Supplementary Figure 11. Freezing and USV behaviour across extinction training. (A) Grouped data showing the average percentage of time spent freezing during presentation of each CS+ tone as a function of extinction training. Each data point based on average of 7 CS+ presentations per animal ± SEM. Five blocks of extinction (Ext1-5) with early extinction (EE, ext1,2) shaded dark grey, and late extinction (LE, ext4,5), shaded light grey. Control data (blue, n = 9 rats) and DREADD data (red, n = 10 rats). (B) Same as A but during the inter-tone interval (ITI). (C) Same as A but grouped data showing average count of USVs emitted during each CS+ presentation as a function of extinction training. Control (blue, n = 9 rats) and DREADD (red, n = 10 rats) (D) Same as C but average USV count during the ITI. Mean ± SEM.

UOB Confidential